Univ. Prof. Ansgar Jüngel

TECHNISCHE UNIVERSITÄT WIEN

DIPLOMARBEIT

NONLINEAR POISSON-NERNST-PLANCK EQUATIONS FOR ION FLUX THROUGH CONFINED CHANNELS

Ausgeführt am
INSTITUTE FOR ANALYSIS
AND SCIENTIFIC COMPUTING
der
TECHNISCHE UNIVERSITÄT WIEN

unter der Anleitung von
UNIV. PROF. ANSGAR JÜNGEL
DIPL. ING. ANITA GERSTENMAYER

durch
CHRISTIAN AUMAYR, BSC.
Mahlergasse 4, 3100 St. Pölten

Wien, August 2016

Christian Aumayr

Christian Aumayr: *Nonlinear Poisson-Nernst-Planck equations for ion flux through confined channels,* Master Thesis, © August 2016

SUPERVISORS:
Univ. Prof. Ansgar Jüngel
Dipl. Ing. Anita Gerstenmayer

LOCATION:
Wien

TIME FRAME:
März 2016 - August 2016

Mathematics is the language
in which God has written the universe.

— Galileo Galilei 1564-1642

ABSTRACT

In recent years mathematical models for ion flux through confined channels have become of broad interest with various applications in biophysics, biochemistry and physiology. While the standard models, one of them being the Poisson-Nernst-Planck (PNP) model, for these problems deal very well with the electrostatic interactions, effects on the flux due to crowding inside the channel are widely neglected. For channel dimensions much larger than the ion size it can be argued that such an approach is reasonable, but with decreasing channel size crowding effects due to volume exclusion in the channel have to be taken into consideration. In a recent paper M. Burger et al. introduced a modified PNP-model with nonlinear mobility to include such effects. In this Thesis we show the derivation of said model from a self consistent random walk model and investigate transformation into entropy variables and existence for stationary solutions. Furthermore we showcase a reduction in dimension for faster computing speed and implement it in Matlab. In the last chapter we verify the derived results, by conducting a series of tests and comparing them to literature.

KURZFASSUNG

Die Beschreibung von Ionenflüssen durch enge Ionenkanäle ist ein aktuelles Forschungsgebiet in diversen naturwissenschaftlichen Bereichen wie etwa Biophysik, Biochemie und Physiologie. Die mathematischen Standardmodelle in diesem Bereich, z.B. das Poisson-Nernst-Planck Model, sind für die elektrostatischen Wechselwirkungen in besagten Vorgängen bereits sehr gut entwickelt, vernachlässigen jedoch jegliche Effekte die durch Volumenverdrängung in sehr engen Kanälen entstehen. Dieser Zugang liefert gute Ergebnisse solange der Durchmesser der Ionen relativ "klein" im Vergleich zu den Dimensionen des Kanals ist. Bei sehr kleinen Ionenkanälen müssen diese Effekte berücksichtigt werden. In einer aktuellen Publikation stellen M. Burger et al. ein Model mit nichtlinearer Mobilität vor, das diese Volumenverdrängung berücksichtigt. In dieser Diplomarbeit führen wir die Herleitung dieses Modelles und einen Existenzbeweis für stationäre Lösungen, durch geschickte Transformation in sogenannte Entropievariablen vor. Außerdem wird eine Dimensionsreduktion auf des Problems 1D durchgeführt und diese als Matlab Code implementiert. Im letzten Kapitel verifizieren wir die damit erhaltenen Ergebnisse durch eine Reihe von Testrechnungen und Vergleich mit entsprechenden Literaturergebnissen.

"Ever tried. Ever failed. No Matter.
Try again. Fail again. Fail better."

– Samuel Beckett

ACKNOWLEDGEMENTS

I would like to seize the opportunity and thank all the people that were crucial during the course of my diploma thesis. First and foremost my Professor and Mentor Ansgar Jüngel who introduced me to work on nonlinear Poisson Nernst Planck equations and awakened my interest in research of PDEs in general. Thank you! I am grateful for the chance to work on such a thrilling topic.

Very special thanks also go out to my direct supervisor Anita Gerstenmayer. She taught me a great deal on how to work scientifically and showed me the positive and thrilling sides as well as helping me through the sometimes tiresome. Many thanks for proofreading my thesis and all the improvements and suggestions you added.

I would also like to thank all my university colleagues for their input and support on my thesis as well as all the members of the group for "Atomic and Plasma Physics" at the IAP, for making every coffee brake memorable and generally accepting me as one of theirs.

Last but not the least, I would like to thank my family and friends. My brother and sister for supporting me in spirit throughout the writing of this thesis and my life in general and especially my parents for guiding, supporting and encouraging me throughout the course of my life and for rendering my eduction possible in the first place.

CONTENTS

I MODELING 1

1 INTRODUCTION 3
- 1.1 Ion channels . . . 3
- 1.2 Classical Poisson-Nernst-Planck model . . . 3
- 1.3 Organization of this thesis . . . 4

2 DERIVATION OF THE MODIFIED PNP MODEL 5
- 2.1 1D hopping model . . . 5
- 2.2 Entropy . . . 8
- 2.3 Modified PNP model . . . 9
  - 2.3.1 Scaling . . . 10
  - 2.3.2 Boundary conditions . . . 10
- 2.4 Transformation to entropy variables . . . 11

3 REDUCTION TO 1D 13
- 3.1 Model assumptions . . . 13
- 3.2 Reduction to one dimension . . . 13

II ANALYSIS 19

4 EXISTENCE PROOF 21

III NUMERICS 29

5 NUMERICAL IMPLEMENTATION 31
- 5.1 Further model assumptions . . . 31
- 5.2 Solving method . . . 32

6 RESULTS, TESTS AND OUTLOOK 35
- 6.1 Sample calculation . . . 35
- 6.2 Several tests . . . 36
  - 6.2.1 Numerical convergence test . . . 36
  - 6.2.2 Residual error test . . . 37
  - 6.2.3 Peak maximum . . . 38
- 6.3 Summary and outlook . . . 42

IV APPENDIX 43

A THEOREMS AND DEFINITIONS 45

BIBLIOGRAPHY 49

LIST OF FIGURES

Figure 1 Experimental Setup (figure taken from [6]) . . 11
Figure 2 Scetch of the channel (figure taken from [6]) . 13
Figure 3 Oxygen profile with linear interpolation 36
Figure 4 Unscaled concentration profiles 37
Figure 5 Unscaled potential profile 38
Figure 6 Crowding effects inside the channel 38
Figure 7 Estimated numerical errors 39
Figure 8 Estimated residuals 40
Figure 9 Sketch of piecewise linear oxygen profile . . . 41
Figure 10 Sketch of piecewise constant oxygen profile . 41
Figure 11 Semilogplot for peak size over the maximal gradient in the oxygen concentration in Ca^{2+} 41
Figure 12 Semilogplot for peak size over the maximal gradient in the oxygen concentration in Na^{+} . 41

LIST OF TABLES

Table 1 Physical parameters cf. [7] 32
Table 2 Model assumptions cf. [7] 32
Table 3 Unscaled and untransformed boundary conditions 35

GLOSSARY

SPECIAL SETS:

$\mathbb{R}$	Set of real numbers

SPECIAL SYMBOLS:

$\mathbb{P}(A)$	Probability of A
$\mathcal{R}(u)$	Residuum of u
$\delta F(u_0, \xi)$	First Variation of F(u) at u_0 in the direction of ξ
Ω	Usually the geometry in question
$\partial\Omega$	The boarder of said geometry
$\gamma_0(.)$	the trace operator on $H^1(\Omega)$ as defined in [1]
$(.,.)_{\mathbb{H}}$	Scalar product of Hilbert space $\mathbb{H}$
$\text{meas}(A)$	Lebesgue measure of the set $A \subseteq \mathbb{R}^n$
$(V > M)$	V and M being maps from Ω to $\mathbb{R}$: $(V > M) = \{x \in \Omega \mid V(x) > M(x)\}$
$f = \mathcal{O}(g)$	g is an asymptotically upper bound to f
V^*	the dual space of V

FUNCTION SPACES:

$L^p(\Omega)$	Space of p-integrable real valued functions
$W^{k,p}(\Omega)$	Sobolev Space of real valued functions with derivates in $L^p(\Omega)$ up to order k
$W_0^{k,p}(\Omega)$	Subspace of $W_0^{k,p}(\Omega)$ containing functions with trace zero
$H^k(\Omega)$	Sobolev Space $W^{k,2}(\Omega)$
$H_0^k(\Omega)$	Sobolev Space $W_0^{k,2}(\Omega)$
$H^{\frac{1}{2}}(\partial\Omega)$	$\gamma_0(H^1(\Omega))$ with the norm $\|u\|_{H^{\frac{1}{2}}(\partial\Omega)} := \inf_{U \in H^1(\Omega), \gamma_0(U)=u} \|U\|_{H^1(\Omega)}$

ACRONYMS

i.e.	id est (that is)
cf.	conferre (compare)
a.e.	almost everywhere
w.l.o.g.	without loss of generality
w.r.t.	with respect to
PNP	Poisson-Nernst-Planck
FEM	finite element method
FDM	finite difference method

Part I

MODELING

In the first part of the thesis we will introduce the reader to the standard linear PNP-Model and discuss why and when there might be a need for a modified model. We will derive such a model from a 1D hopping model and investigate transformation to so called entropy variables. Finally we will work on a reduction of dimension for our problem for easier implementation and faster computing speed.

1 INTRODUCTION

Selective transport of atomic or molecular ions through nano-sized channels or pores is currently of broad interest in different scientific fields. Transport mechanisms are expected to change dramatically if the pore dimension is reduced to the nanometer scale and becomes comparable to molecular dimensions [2]. A better understanding of the selectivity of ion transport through nano channels might lead to new applications and devices like molecular sieves [3], ultrafilters [4] or biosensors [5].

This work is concerned with modeling the transport of ions through confined geometries in particular ion channels. Due to the limited space and the amount of particles involved, crowding effects due to the actual particle size have to be taken into consideration. As a starting point we work with a model introduced in [6] and recap some results established in [7]. Then we implement a 1D reduction of the model in Matlab and verify our numerical results by a series of tests as well as comparison to existing simulations.

1.1 ION CHANNELS

The movement of ions through confined ion channels is an interesting problem investigated by physicists, chemists and biologists alike. The most popular application are being presented by living cells themselves. Being enveloped by lipid membranes nearly impermeable to physiological ions (e.g. Na^+, K^+, Ca^{2+}, Cl^-), ion exchange almost only happens through so called open ion channels, proteins embedded in the membrane that form ion-selective pores [8]. These ion channels control many vital functions in biology like the forwarding of action potentials in nerve fibers, the contraction of muscles, the regulation of blood pressure to name just a few.

1.2 CLASSICAL POISSON-NERNST-PLANCK MODEL

Walther Nernst was a German physicist, chemist and nobel prize winner in the late 19th to the early 20th century who among other things was one of the first to research the role of ion channels in physiological processes [9–11]. He was also the one who together with Max Plank formulated the Nernst-Plank equations [12], a basic model for electro diffusion

$$\partial_t c_i = \nabla \cdot \left(D_i (\nabla c_i + \mu_i c_i (e z_i \nabla V + \nabla W_i^0)) \right),$$

in some domain Ω where c_i denotes the ion concentration, $i = 1 \dots M$, with M being the number of different ions with charges z_i, diffusion coefficients D_i and mobilities μ_i. V is the electrical and W_i^0 the external potential and e denotes the elementary charge [6]. Together with the Poisson equation

$$-\nabla \cdot (\epsilon \nabla V) = e(\sum_j z_j c_j + f),$$

where ϵ and f denote the permittivity and a charge density respectively [6], the so called PNP-Model (Poisson-Nernst-Planck) becomes a self consistent and widely used electro-diffusion model that can be used to describe ion flux through single ion channels. This model however treats ions as point particles without volume, which works well with "large" channels and "small" ions. If however the channel dimensions become comparable to the particle size, the results of said model become questionable as crowding effects inside the channel are unaccounted for [7].

1.3 ORGANIZATION OF THIS THESIS

The remainder of this thesis is organized as follows:

In Chapter 2, we derive a modified nonlinear PNP-Model from a 1D hopping model, that is effected by volume exclusion and crowding effects. We also investigate scaling as well as transformation to so called entropy variables which we will need in Chapter 4.

In Chapter 3, we introduce a dimensional reduction of our modified PNP-Model to 1D, for easier computing.

In Chapter 4, we outline an existence proof for our stationary modified model.

In Chapter 5, we describe our numerical implementation of the modified model

In Chapter 6, we validate our numerical implementation by comparison to other results and performing a series of tests Then we give an outlook on possible future extensions of the model.

2

DERIVATION OF THE MODIFIED PNP MODEL

A frequently used model to describe ion flow through narrow pores is the standard PNP model with linear mobility (cf [13]). As already stated in chapter 1 the validity of such a model is at least doubtful for very large volume densities, since one would expect saturation because of volume filling. In the following chapter we will derive a modified PNP model with nonlinear mobilities from a microscopic lattice-based model with volume exclusion which we have adapted from [7]. This model will be the basis for our further investigations.

2.1 1D HOPPING MODEL

Let $\mathcal{T}_h$ denote an equidistant 1 dimensional grid of element size h. Every point on the grid can only be occupied by a single particle at a given time t. Let further $c_i(x,t)$ be the probability of finding a particle of species i and charge z_i at time t at location x

$$c_i(x,t) = \mathbb{P}(\text{particle of species } i \text{ is at time } t \text{ at position } x).$$

We assume that particles of species i evolve according to diffusion and a scaled potential $W_i(x,t)$. The transition rates

$$\begin{aligned}&\widetilde{\Pi}^+_{c_i}(x,t)\\ =&\mathbb{P}(\text{particle of species } i \text{ jumps from position } x \text{ to } x+h \text{ in } (t,t+\Delta t)),\\ &\widetilde{\Pi}^-_{c_i}(x,t)\\ =&\mathbb{P}(\text{particle of species } i \text{ jumps from position } x \text{ to } x-h \text{ in } (t,t+\Delta t))\end{aligned}$$

accordingly become

$$\begin{aligned}\widetilde{\Pi}^+_{c_i}(x,t) &= \alpha_i \exp(-\beta(W_i(x+h)-W_i(x))),\\ \widetilde{\Pi}^-_{c_i}(x,t) &= \alpha_i \exp(-\beta(W_i(x-h)-W_i(x))),\end{aligned}$$

where β denotes the mobility constant and α_i denote the normalization constants for the probability density [7]. Now considering the goal of this model to include volume exclusion we take into account that the neighboring sites might be occupied. This assumption is included in the model by

$$\begin{aligned}\Pi^+_{c_i}(x,t) &= \widetilde{\Pi}^+_{c_i}(x,t)\cdot\mathbb{P}(\text{position } x+h \text{ is at time } t \text{ not occupied}),\\ \Pi^-_{c_i}(x,t) &= \widetilde{\Pi}^-_{c_i}(x,t)\cdot\mathbb{P}(\text{position } x-h \text{ is at time } t \text{ not occupied}).\end{aligned}$$

The closure assumption that a site is free is

$$\mathbb{P}(\text{position } x \text{ is at time } t \text{ not occupied}) = 1-\sum_i c_i(x,t).$$

which corresponds to rigorous results for a single species [14]. The probability to find a particle of species i at position x at time $t+\Delta t$ is given by the probability of a particle being there at time t subtracted by the chance of said particle moving away in the given time and adding the probability of a particle of said species moving toward position x in Δt

$$\begin{aligned} c_i(x,t+\Delta t) = c_i(x,t)(1-\Pi^+_{c_i}(x,t)-\Pi^-_{c_i}(x,t)) \\ +c_i(x+h,t)\Pi^-_{c_i}(x+h,t)+c_i(x-h,t)\Pi^+_{c_i}(x-h,t). \end{aligned}$$

This transforms after small manipulation into

$$\begin{aligned} c_i(x,t+\Delta t)-c_i(x,t) = \\ c_i(x,t)\left(\Pi^+_{c_i}(x-h,t)+\Pi^-_{c_i}(x+h,t)-\Pi^+_{c_i}(x,t)-\Pi^-_{c_i}(x,t)\right) \\ +\left(c_i(x+h,t)-c_i(x,t)\right)\Pi^-_{c_i}(x+h,t) \\ +\left(c_i(x-h,t)-c_i(x,t)\right)\Pi^+_{c_i}(x-h,t). \end{aligned}$$

Taylor expansions of $c_i(x+h,t)-c_i(x,t)$, $c_i(x-h,t)-c_i(x,t)$ as well as $\Pi^+_{c_i}(x-h,t)+\Pi^-_{c_i}(x+h,t)$ in h up to second order at $h=0$ yields

$$\begin{aligned} &c_i(x,t+\Delta t)-c_i(x,t) = \\ &c_i(x,t)\Bigg(h\cdot\underbrace{\partial_x\left(\Pi^-_{c_i}(x,t)-\Pi^+_{c_i}(x,t)\right)}_{①}+\frac{h^2}{2}\cdot\underbrace{\partial_{xx}\left(\Pi^+_{c_i}(x,t)+\Pi^-_{c_i}(x,t)\right)}_{②}\Bigg) \\ &+h\cdot\partial_x c_i(x,t)\underbrace{\left(\Pi^-_{c_i}(x+h)-\Pi^+_{c_i}(x-h,t)\right)}_{③} \\ &+\frac{h^2}{2}\cdot\partial_{xx}c_i(x,t)\underbrace{\left(\Pi^-_{c_i}(x+h,t)+\Pi^+_{c_i}(x-h,t)\right)}_{④}+\mathcal{O}(h^3). \end{aligned} \tag{1}$$

In order to evaluate ①, ②, ③ and ④ we are going to use Taylor's expansion once again on the transition rates

$$\begin{aligned} \Pi^+_{c_i}(x,t) = \alpha_i\big(1-\sum_j c_j(x,t)\big) \\ -h\Big(\beta_i\partial_x W_i(x,t)\big(1-\sum_j c_j(x,t)\big)+\alpha_i\sum_j\partial_x c_j(x,t)\Big) \\ +\mathcal{O}(h^2), \end{aligned}$$

$$\begin{aligned} \Pi^-_{c_i}(x,t) = \alpha_i\big(1-\sum_j c_j(x,t)\big) \\ +h\Big(\beta_i\partial_x W_i(x,t)\big(1-\sum_j c_j(x,t)\big)+\alpha_i\sum_j\partial_x c_j(x,t)\Big) \\ +\mathcal{O}(h^2), \end{aligned}$$

$$\Pi^{-}_{c_i}(x+h,t) = \alpha_i\big(1-\sum_j c_j(x,t)\big) \\ -h\beta_i\partial_x W_i(x,t)\big(1-\sum_j c_j(x,t)\big)+\mathcal{O}(h^2),$$

$$\Pi^{+}_{c_i}(x-h,t) = \alpha_i\big(1-\sum_j c_j(x,t)\big) \\ +h\beta_i\partial_x W_i(x,t)\big(1-\sum_j c_j(x,t)\big)+\mathcal{O}(h^2),$$

with $\beta_i := \alpha_i \cdot \beta$. Now we have

$$\begin{aligned}
&① : \partial_x\Pi^{-}_{c_i}(x,t) - \partial_x\Pi^{+}_{c_i}(x,t) &&= 2h\beta_i\partial_x\Big(\partial_x W_i(x,t)\big(1-\sum_j c_j(x,t)\big)\Big) \\
&&&\quad +2h\alpha_i\sum_j \partial_{xx}c_j(x,t)+\mathcal{O}(h^2),\\
&② : \partial_{xx}\Pi^{+}_{c_i}(x,t) + \partial_{xx}\Pi^{-}_{c_i}(x,t) &&= -2\alpha_i\sum_j \partial_{xx}c_j(x,t)+\mathcal{O}(h^2),\\
&③ : \Pi^{-}_{c_i}(x+h,t) - \Pi^{+}_{c_i}(x-h,t) &&= 2h\beta_i\partial_x W_i(x,t)\big(1-\sum_j c_j(x,t)\big) \\
&&&\quad +\mathcal{O}(h^2),\\
&④ : \Pi^{-}_{c_i}(x+h,t) + \Pi^{+}_{c_i}(x-h,t) &&= 2\alpha_i\big(1-\sum_j c_j(x,t)\big)+\mathcal{O}(h^2).
\end{aligned}$$

Putting those expressions into equation (1) we get

$$\begin{aligned}
c_i(x,t+\Delta t) - c_i(x,t) &= 2h^2\beta_i c_i(x,t)\partial_x\Big(\partial_x W_i(x,t)\big(1-\sum_j c_j(x,t)\big)\Big) \\
&\quad +h^2\alpha_i c_i(x,t)\sum_j \partial_{xx}c_j(x,t) + h^2\alpha_i\partial_{xx}c_i(x,t)\big(1-\sum_j c_j(x,t)\big) \\
&\quad +2h^2\beta_i\partial_x c_i(x,t)\partial_x W_i(x,t)\big(1-\sum_j c_j(x,t)\big)+\mathcal{O}(h^3)
\end{aligned}$$

which can be further simplified using the product rule into

$$\begin{aligned}
&c_i(x,t+\Delta t) - c_i(x,t) = \\
&\quad h^2\alpha_i\partial_x\Big(\big(1-\sum_j c_j(x,t)\big)\partial_x c_i(x,t) + c_i(x,t)\sum_j \partial_x c_j(x,t)\Big) \\
&\quad +2h^2\beta_i\partial_x\Big(c_i(x,t)\big(1-\sum_j c_j(x,t)\big)\partial_x W_i(x,t)\Big)+\mathcal{O}(h^3)
\end{aligned}$$

With appropriate scaling $\frac{\alpha_i}{2} \approx D_i$ (D_i being the diffusion coefficient of species i), $\mu = \frac{2\beta_i}{\alpha_i} = 2\beta$ and time step $\Delta t = 2h^2$, letting t go to

zero and evaluating all expressions at (x,t) if not further specified the resulting system of differential equations becomes

$$\partial_t c_i = D_i \partial_x \Big((1 - \sum_j c_j) \partial_x c_i + c_i \sum_j \partial_x c_j + \mu c_i (1 - \sum_j c_j) \partial_x W_i \Big) \tag{2}$$

A multidimensional derivation can be done analogously [6]. Further denoting the volume density $\sum_j c_j(x,t)$ by ρ this reads

$$\partial_t c_i = D_i \nabla \big((1-\rho) \nabla c_i + c_i \nabla \rho + \mu c_i (1-\rho) \nabla W_i \big). \tag{3}$$

2.2 ENTROPY

The entropy $E(x,t)$ of (3) is defined via

$$\begin{aligned} E(x,t) = \int \sum_i \big(c_i(x,t) \log(c_i(x,t)) \big) + (1-\rho(x,t)) \log(1-\rho(x,t)) \\ + \sum_i \mu_i c_i(x,t) W_i(x,t) \, dx \end{aligned}$$

[7]. For further investigation of the time evolution of the entropy we first introduce so called entropy variables (cf [15, 16] and chapter 2.4)

$$u_i(x,t) = \partial_{c_i} E(x,t) + \text{const.},$$

where ∂_{c_i} has to be interpreted as the variational derivative of $E(x,t)$ w.r.t. c_i. For any eligible ξ the first variation of $E(x,t)$ w.r.t. c_i in direction of ξ is given by

$$\begin{aligned} \delta E(c_i, \xi) &= \frac{d}{d\epsilon} \int_\Omega \sum_i \big(c_i + \epsilon\xi \big) \log(c_i + \epsilon\xi) + \mu_i (c_i + \epsilon\xi) W_i \big) \\ &\quad + (1 - \rho - \epsilon\xi) \log(1 - \rho - \epsilon\xi) \, dx \Big|_{\epsilon=0} \\ &= \int_\Omega \xi \log(c_i + \epsilon\xi) - \xi \log(1 - \rho - \epsilon\xi) + \xi \mu_i W_i \, dx \Big|_{\epsilon=0} \\ &= \int_\Omega \big(\log(c_i) - \log(1-\rho) + \mu_i W_i \big) \cdot \xi \, dx \end{aligned}$$

The entropy variables therefore become

$$u_i = \log(c_i) - \log(1-\rho) + \mu_i W_i. \tag{4}$$

Now we look at the time derivative of E(x,t) under the assumption that $\partial_t W_i(x,t) = 0$.

$$\begin{aligned}\partial_t E &= \int_\Omega \sum_i \big((\partial_t c_i)\log(c_i) + \partial_t c_i\big) \\ &\qquad -(\partial_t \rho)\log(1-\rho) - \partial_t \rho + \sum_i (\partial_t c_i)\mu_i W_i \,dx \\ &= \int_\Omega \sum_i \big((\partial_t c_i)\log(c_i) - (\partial_t c_i)\log(1-\rho) + (\partial_t c_i)\mu_i W_i\big)\,dx \\ &= \int_\Omega \sum_i (\partial_t c_i)u_i \,dx\end{aligned}$$

Using equation (3) and the fact that

$$D_i c_i(1-\rho)\nabla u_i = D_i(1-\rho)\nabla c_i + D_i c_i \nabla \rho + D_i c_i(1-\rho)\mu_i \nabla W_i$$

we further get

$$\partial_t E = \int_\Omega \sum_i \nabla \cdot \big(D_i c_i(1-\rho)\nabla u_i\big)u_i \,dx.$$

Under the reasonable assumption of no-flux boundary conditions, i.e. when investigating a closed system this can be further transformed into

$$\partial_t E = -\int_\Omega \sum_i \big(D_i c_i(1-\rho)|\nabla u_i|^2\big)\,dx.$$

Since $0 \leqslant c_i \leqslant 1, 0 < D_i$ and $0 \leqslant \rho \leqslant 1$ we can conclude that in a closed system the entropy decreases in time as is expected from a model that describes physical phenomena. Similar arguments are true if $\partial_t W_i \neq 0$, but satisfies the Poisson equation [7, 17], i.e. in our modified PNP-Modell if $W_i^0 = 0$ (cf. chapter 2.3).

2.3 MODIFIED PNP MODEL

Following the motivation for our modified Nernst-Planck equation, we supplement it with the Poisson equation in order to obtain a self-consistent model. It is used to calculate the potential $V(x,t)$ for charged particles [6]

$$-\epsilon \partial_{xx} V(x,t) = e\big(\sum_j z_j c_j(x,t) + f(x)\big). \tag{5}$$

where ϵ and e denote the permittivity and elementary charge respectively, while f denotes the permanent charge density and z_i the ion charge. In addition to the electrostatic potential, an external potential W_i^0 is used to model any external forces. With $W_i(x,t) =$

$z_i eV(x,t) + W_i^0(x,t)$ our modified PNP Model (suppressing (x,t)) becomes

$$-\epsilon\Delta V = e\Big(\sum_j z_j c_j + f\Big) \tag{6}$$

$$\begin{aligned}\partial_t c_i = \nabla\cdot\Big(D_i\big((1-\rho)\nabla c_i + c_i\nabla\rho + ez_i\mu_i c_i(1-\rho)\nabla V \\ +\mu_i c_i(1-\rho)\nabla W_i^0\big)\Big)\end{aligned} \tag{7}$$

2.3.1 *Scaling*

Before investigating any properties of those equations we transform them into appropriately scaled and dimensionless versions. Given a typical length $\tilde{L}$, voltage $\tilde{V}$ and ion concentration $\tilde{c}$, we define our new variables as

$$x = \tilde{L}x_s, \quad V = \tilde{V}V_s, \quad c_i = \tilde{c}c_{is}, \quad f = \tilde{c}f_s \quad t = \frac{L^2}{\tilde{D}}t_s \quad \text{and}$$
$$D_i = \tilde{D}D_{is}.$$

Plugging this into our model (6) and (7) we get (suppressing the subscript s) the following dimensionless formulation of our model

$$-\lambda^2\Delta V = \sum_j z_j c_j + f \tag{8}$$

$$\begin{aligned}&\partial_t c_i = \nabla\cdot J_i\,, \\ &J_i = D_i((1-\rho)\nabla c_i + c_i\nabla\rho + \eta_i z_i c_i(1-\rho)\nabla V + c_i(1-\rho)\nabla W_i^0)\end{aligned} \tag{9}$$

with some appropriately scaled external potential W_i^0 and

$$\lambda^2 = \frac{\epsilon\tilde{V}}{e\tilde{L}^2\tilde{c}} \quad \text{and} \quad \eta_i = e\tilde{V}\mu_i.$$

J_i is called the flow of the ion species i.

2.3.2 *Boundary conditions*

The investigated geometry Ω will be some subset of $\mathbb{R}^n$ with locally Lipschitz continuous boundaries. The model itself will resemble an experimental setup known as the patch-clamp method (cf. [18]). In that setup there are certain parts were no-flux boundary conditions apply and others where Dirichlet conditions apply i.e. the left and right baths that are used to control the concentration, cf. 1. This can be modelled via:

$$c_i(x,t) = \gamma_i(x) \quad x \in \Gamma_B, \tag{10}$$
$$J_i(x,t)\cdot n = 0 \quad x \in \partial\Omega\backslash\Gamma_B \tag{11}$$

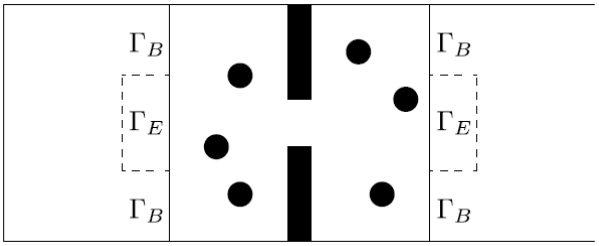

Figure 1: Experimental Setup (figure taken from [6])

We also want to ensure that for the bath concentrations restrictions of charge neutrality apply, i.e.

$$\sum_j z_j \gamma_j(x) = 0 \tag{12}$$

For the Potential we assume that it is only influenced via an applied potential between 2 electrodes, on the remaining parts of $\partial\Omega$ also no flux boundary conditions apply

$$V(x,t) = V_D(x) \quad x \in \Gamma_E, \tag{13}$$
$$\nabla V(x,t) \cdot n = 0 \quad x \in \partial\Omega \backslash \Gamma_E \tag{14}$$

Furthermore we will from now on use the following convention

$$H^1_{0\Gamma_B}(\Omega) := \{u \in H^1(\Omega) \mid u_{|\Gamma_B} = 0\} \tag{15}$$

2.4 TRANSFORMATION TO ENTROPY VARIABLES

From now on we shall focus mainly on the stationary problem, which is of great interest for computing flow characteristics, e.g. current voltage relations [6]. We remember the scaled stationary problem is given by

$$-\lambda^2 \Delta V = \sum_j z_j c_j + f \tag{16}$$

$$0 = \nabla \cdot \big(D_i((1-\rho)\nabla c_i + c_i \nabla \rho + \eta_i z_i c_i (1-\rho)\nabla V + c_i(1-\rho)\nabla W_i^0)\big) \tag{17}$$

with the boundary conditions (10), (11), (13) and (14). The natural formulation of the problem in concentration variables may not be the best formulation in terms of analysis and computing. In the standard PNP model there are two common transformations, namely the one into entropy variables and the one into so called Slotboom variables [6]. We can now try to apply the former onto our modified problem.

Remembering equation (4) we know that the entropy variables look like this:

$$u_i = \partial_{c_i} E + const = \log c_i - \log(1-\rho) + \eta_i z_i V + W_i^0.$$

To obtain an explicit inversion of this form we first take the exponential form

$$\frac{c_i}{1-\rho} = \exp(u_i - \eta_i z_i V - W_i^0)$$

and use the following identity for $1-\rho$

$$\frac{1}{1+\sum_j \exp(u_j - \eta_j z_j V - W_j^0)} = \frac{1}{1+\sum_j \frac{c_j}{1-\rho}} = \frac{1}{\frac{1-\rho+\rho}{1-\rho}} = 1-\rho$$

and therefore get

$$c_i = \frac{\exp(u_i - \eta_i z_i V - W_i^0)}{1+\sum_j \exp(u_j - \eta_j z_j V - W_j^0)}.$$

Our stationary model (16) and (17) can now be rewritten into

$$-\lambda^2 \Delta V - \frac{\sum_k z_k \exp(u_k - \eta_k z_k V - W_k^0)}{1+\sum_j \exp(u_j - \eta_j z_j V - W_j^0)} = f \tag{18}$$

$$\nabla \cdot \Big(D_i \frac{\exp(u_i - \eta_i z_i V - W_i^0)}{(1+\sum_j \exp(u_j - \eta_j z_j V - W_j^0))^2} \nabla u_i \Big) = 0 \tag{19}$$

One of the attractive features of this transformation is the elimination of cross diffusion, the coupling only occurs in the diffusion coefficients. Hence a maximum principle holds for u_i, cf. [7] and chapter4, obtaining the maximum and minimum at Γ_B with transformed boundary conditions

$$u_i = u_i^D := \log \gamma_i - \log\Big(1 - \sum_j \gamma_j\Big) + \eta_i z_i V_D + W_i^0 \quad x \in \Gamma_B, \tag{20}$$

$$\nabla u_i \cdot n = 0 \qquad x \in \partial\Omega \backslash \Gamma_B \tag{21}$$

3 REDUCTION TO 1D

Since the cross section of an ion channel filter is a lot smaller than the length of the actual channel it is reasonable to try to approximate the three dimensional model by a one dimensional one. Such a model is obviously faster to compute and easier to implement. Again this is an adaptation of similar work in [7].

3.1 MODEL ASSUMPTIONS

Unless otherwise specified the following assumptions hold for the rest of this chapter as well as chapter 5 and 6. We consider an L-type calcium selective ion channel. Its geometry is modeled by a cylinder with radius r_c and length l_c embedded in 2 baths with the shape of truncated cones with length l_b and outer radius r_b. The boundary is split into 2 parts: $\Gamma_B = \Gamma_E = \Gamma_L \cup \Gamma_R$ and $\Gamma_N = \partial\Omega \setminus (\Gamma_L \cup \Gamma_R)$ see figure 2. For our dimension reduction to work we also have to assume that the boundary conditions are constant in y and z directions on Γ_L and Γ_R. We also assume that the external potential W_i^0 is zero.

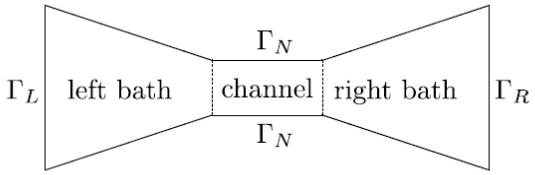

Figure 2: Scetch of the channel (figure taken from [6])

3.2 REDUCTION TO ONE DIMENSION

We model our domain the following way, cf. figure 2:

$$\Omega^\epsilon = \big\{(x, r^\epsilon(x)\cos(\Theta), r^\epsilon(x)\sin(\Theta)) \in \mathbb{R}^3 \\ \big| \; x \in [-L, L],\ 0 \leqslant r^\epsilon(x) \leqslant \epsilon r_0,\ \Theta \in [0, 2\pi)\big\}$$

with r_0 being the typical radius. Now we rescale the dimensional variables $y^\epsilon = \epsilon y$, $z^\epsilon = \epsilon z$, as well as the potential $V^\epsilon(x, y^\epsilon, z^\epsilon) = \tilde{V}^\epsilon(x, y, z)$, densities $c_i^\epsilon(x, y^\epsilon, z^\epsilon) = \tilde{c}_i^\epsilon(x, y, z)$ and transformed densities $u_i^\epsilon(x, y^\epsilon, z^\epsilon) = \tilde{u}_i^\epsilon(x, y, z)$. From the existence proof in chapter 4 we get the following solutions to (18) and (19)

$$V^\epsilon(x, y^\epsilon, z^\epsilon), \quad c_i^\epsilon(x, y^\epsilon, z^\epsilon), \quad u_i^\epsilon(x, y^\epsilon, z^\epsilon) \qquad \in H^1(\Omega^\epsilon) \cap L^\infty(\Omega^\epsilon)$$

bounded in $L^\infty(\Omega)$ uniformly in ϵ and fulfilling the following equations

$$\lambda^2 \int\int\int_{\Omega^\epsilon} \partial_x V^\epsilon \partial_x \phi + \partial_{y^\epsilon} V^\epsilon \partial_{y^\epsilon} \phi + \partial_{z^\epsilon} V^\epsilon \partial_{z^\epsilon} \phi \, dx \, dy^\epsilon dz^\epsilon = \int\int\int_{\Omega^\epsilon} \Big(\sum_j z_j c_j^\epsilon + f \Big) \phi \, dx \, dy^\epsilon dz^\epsilon, \tag{22}$$

$$\int\int\int_{\Omega^\epsilon} D_i \frac{\exp(u_i^\epsilon - \eta_k z_k V^\epsilon)}{(1 + \sum_j \exp(u_j^\epsilon - \eta_j z_j V^\epsilon))^2} \nabla u_i^\epsilon \nabla \phi \, dx \, dy^\epsilon dz^\epsilon = 0 \tag{23}$$

with $\phi \in H_0^1(\Omega)$ and also fulfilling the boundary conditions (20), (21), (13) and (14). First we look at the Poisson equation (22), substituting y for y^ϵ and z for z^ϵ. We obtain

$$\lambda^2 \epsilon^2 \int\int\int_{\Omega^1} \partial_x \tilde{V}^\epsilon \partial_x \tilde{\phi} + \frac{1}{\epsilon^2} \partial_y \tilde{V}^\epsilon \partial_y \tilde{\phi} + \frac{1}{\epsilon^2} \partial_z \tilde{V}^\epsilon \partial_z \tilde{\phi} \, dx \, dy \, dz = \epsilon^2 \int\int\int_{\Omega^1} \Big(\sum_j z_j \tilde{c}_j^\epsilon + f \Big) \tilde{\phi} \, dx \, dy \, dz. \tag{24}$$

Taking the special test function $\tilde{\phi}(x, y, z) = \tilde{V}^\epsilon(x, y, z) - g(x)$ with $g(x)$ being a linear function of x in $[-L, L]$ so that $\tilde{\phi}$ vanishes at $x = \pm L$, we get

$$\begin{aligned} &\lambda^2 \int\int\int_{\Omega^1} \partial_x \tilde{V}^\epsilon \partial_x (\tilde{V}^\epsilon - g) + \frac{1}{\epsilon^2} |\partial_y \tilde{V}^\epsilon|^2 + \frac{1}{\epsilon^2} |\partial_z \tilde{V}^\epsilon|^2 \, dx \, dy \, dz \\ &\qquad = \int\int\int_{\Omega^1} \Big(\sum_j z_j \tilde{c}_j^\epsilon + f \Big) (\tilde{V}^\epsilon - g) \, dx \, dy \, dz \\ &\leqslant \Big(\sum_j |z_j| \|\tilde{c}_j^\epsilon\|_{L^\infty(\Omega^1)} + \|f\|_{L^\infty(\Omega^1)} \Big) \|\tilde{V}^\epsilon - g\|_{L^\infty(\Omega^1)} |\Omega^1| \leqslant k. \end{aligned}$$

with some constant k. Furthermore

$$\begin{aligned} &\lambda^2 \int\int\int_{\Omega} \partial_x \tilde{V}^\epsilon \, \partial_x g \, dx \, dy \, dz \\ &\qquad = \frac{g(L) - g(-L)}{2L} \int\int \tilde{V}^\epsilon(L, y, z) - \tilde{V}^\epsilon(-L, y, z) \, dy \, dz \end{aligned}$$

and therefore

$$\lambda^2 \int\int\int_{\Omega_1} (\partial_x \tilde{V}^\epsilon)^2 + \frac{1}{\epsilon^2} (\partial_y \tilde{V}^\epsilon)^2 + \frac{1}{\epsilon^2} (\partial_z \tilde{V}^\epsilon)^2) \, dx \, dy \, dz \leqslant k_1$$

for some other constant k_1 independent of ϵ. Thus

$$\int\int\int_{\Omega_1} (\partial_y \tilde{V}^\epsilon)^2 \, dx \, dy \, dz \leqslant \epsilon^2 k_1 \text{ and } \int\int\int_{\Omega_1} (\partial_z \tilde{V}^\epsilon)^2 \, dx \, dy \, dz \leqslant \epsilon^2 k_1$$

as well as

$$\int\int\int_{\Omega_1} (\partial_x \tilde{V}^\epsilon)^2 \, dx \, dy \, dz \leqslant k_1. \tag{25}$$

Now for $\epsilon \to 0$ we get

$$\|\partial_y \tilde{V}^\epsilon\|_{L^2(\Omega_1)} \to 0 \quad \text{and} \quad \|\partial_z \tilde{V}^\epsilon\|_{L^2(\Omega_1)} \to 0$$

and an overall uniform boundedness of $\nabla \tilde{V}^\epsilon$ in $L^2(\Omega)$ and with Poincaré's inequality A.7 also in $H^1(\Omega^1)$. With the theorem of Eberlein-Šmulian A.1 we get weak convergence along a subsequence $\tilde{V}^\epsilon(x,y,z) \rightharpoonup V^0(x,y,z)$ in $H^1(\Omega^1)$ for $\epsilon \to 0$. Our strong L^2 convergence of $\partial_y \tilde{V}^\epsilon$ and $\partial_z \tilde{V}^\epsilon$ implies also weak convergence and the uniqueness of the limit directly translates into $\partial_y V^0(x,y,z) = 0$ and $\partial_z V^0(x,y,z) = 0$ or $\tilde{V}^\epsilon(x,y,z) \rightharpoonup V^0(x)$ in $H^1(\Omega^1)$ which implies $\partial_x \tilde{V}^\epsilon(x,y,z) \rightharpoonup \partial_x V^0(x)$ in $L^2(\Omega^1)$.

Now we will try to get a similar result for $\tilde{u}_i^\epsilon$ and $\tilde{c}_i^\epsilon$ using the Nernst-Planck equation (23). Transforming again from y^ϵ, z^ϵ to y and z we obtain

$$\begin{aligned}\int\int\int_{\Omega^1} & D_i \frac{\exp(\tilde{u}_i^\epsilon - \eta_i z_i \tilde{V}^\epsilon)}{\left(1 + \sum_j \exp(\tilde{u}_j^\epsilon - \eta_j z_j \tilde{V}^\epsilon)\right)^2} \\ & \cdot \left(\partial_x \tilde{u}_i^\epsilon \partial_x \tilde{\phi} + \frac{1}{\epsilon^2} \partial_y \tilde{u}_i^\epsilon \partial_y \tilde{\phi} + \frac{1}{\epsilon^2} \partial_z \tilde{u}_i^\epsilon \partial_z \tilde{\phi}\right) \epsilon^2 \, dx\, dy\, dz = 0. \quad (26)\end{aligned}$$

Next we can use the uniform boundedness of $\tilde{V}^\epsilon$ and $\tilde{u}^\epsilon$ to deduce that

$$\begin{aligned}0 < k_2 \leqslant \tilde{c}_i^\epsilon &= \frac{\exp(\tilde{u}_i^\epsilon - \eta_i z_i \tilde{V}^\epsilon)}{\left(1 + \sum_j \exp(\tilde{u}_j^\epsilon - \eta_j z_j \tilde{V}^\epsilon)\right)} \\ &\leqslant \frac{\exp(\tilde{u}_i^\epsilon - \eta_i z_i \tilde{V}^\epsilon)}{\left(1 + \sum_j \exp(\tilde{u}_j^\epsilon - \eta_j z_j \tilde{V}^\epsilon)\right)^2} \leqslant k_3. \quad (27)\end{aligned}$$

With test function $\phi(x,y,z) = \tilde{u}_i^\epsilon - g(x)$, with $g(x)$ again being the linear interpolator of $\tilde{u}^\epsilon$ in the vertices $x = \pm L$ we now have

$$\begin{aligned}&\int\int\int_{\Omega^1} D_i k_2 \left(\partial_x \tilde{u}_i^\epsilon \partial_x (\tilde{u}_i^\epsilon - g) + \frac{1}{\epsilon^2} (\partial_y \tilde{u}_i^\epsilon)^2 + \frac{1}{\epsilon^2} (\partial_z \tilde{u}_i^\epsilon)^2\right) \leqslant 0 \\ &\int\int\int_{\Omega^1} D_i k_2 \left((\partial_x \tilde{u}_i^\epsilon)^2 + \frac{1}{\epsilon^2} (\partial_y \tilde{u}_i^\epsilon)^2 + \frac{1}{\epsilon^2} (\partial_z \tilde{u}_i^\epsilon)^2\right) \\ &\qquad \leqslant \frac{g(L) - g(-L)}{2L} \int\int_{\Omega^1} \tilde{u}_i^\epsilon(L,y,z) - \tilde{u}^\epsilon(-L,y,z) \, dy\, dz \leqslant k_4.\end{aligned}$$

We can now see that for $\epsilon \to 0$ we again get

$$\|\partial_y \tilde{u}_i^\epsilon\|_{L^2(\Omega_1)} \to 0 \quad \text{and} \quad \|\partial_z \tilde{u}_i^\epsilon\|_{L^2(\Omega_1)} \to 0$$

as well as uniform boundedness of $\tilde{u}_i^\epsilon$ in $H_0^1(\Omega)$ and using the same arguments as for $\tilde{V}^\epsilon$ we thus get

$$\tilde{u}_i^\epsilon(x,y,z) \rightharpoonup u_i^0(x) \quad \text{in } H^1(\Omega^1)$$

along a subsequence. This leads to strong convergence in $L^2(\Omega)$, point wise convergence a.e. and remembering (27) and the dominated convergence theorem A.2 to strong $L^2(\Omega)$ convergence of $\tilde{c}_i^\epsilon(x,y,z) \to c(x)_i^0$. We can now go back to reducing the dimension of our equation. Taking (24), choosing a test function $\tilde{\phi}(x,y,z) = \tilde{\phi}(x)$ and letting ϵ go to zero we have for the left side of the equation

$$\begin{aligned}\lim_{\epsilon\to 0} \lambda^2 \int\int\int_{\Omega^1} \partial_x \tilde{V}^\epsilon(x,y,z)\partial_x\tilde{\phi}(x)\,dx\,dy\,dz &= \lim_{\epsilon\to 0} \lambda^2 \big(\partial_x \tilde{V}^\epsilon, \partial_x\tilde{\phi}(x)\big)_{L^2(\Omega^1)} \\ &= \lambda^2 \big(\partial_x V^0, \partial_x\tilde{\phi}(x)\big)_{L^2(\Omega^1)} = \lambda^2 \int_{-L}^{L} \partial_x V^0(x)\partial_x\tilde{\phi}(x) \underbrace{\int\int dy\,dz}_{=a(x)}\,dx\end{aligned}$$

where $a(x)$ is defined as the area of the cross section of Ω^1 at x. For the right hand side we get

$$\begin{aligned}&\lim_{\epsilon\to 0}\int\int\int_{\Omega^1} \big(\sum_j z_j\tilde{c}_j^\epsilon + f(x)\big)\tilde{\phi}(x)\,dx\,dy\,dz \\ &\qquad= \lim_{\epsilon\to 0}\big(\sum_j z_j\tilde{c}_j^\epsilon(x,y,z) + f(x), \tilde{\phi}(x)\big)_{L^2(\Omega^1)} \\ &\qquad= \big(\sum_j z_j c_j^0(x) + f(x), \tilde{\phi}(x)\big)_{L^2(\Omega^1)} \\ &\qquad= \int_{-L}^{L} \big(\sum_j z_j c_j^0(x) + f(x)\big)\tilde{\phi}(x) \underbrace{\int\int dy\,dz}_{=a(x)}\,dx.\end{aligned}$$

Going back to a strong formulation we get the full one dimensional Poisson equation (surpressing any index ^{0})

$$-\lambda^2\partial_x\big(a(x)\partial_x V(x)\big) = a(x)\big(\sum_j z_j c_j(x) + f(x)\big). \tag{28}$$

For the Nernst-Planck equation (26) we proceed in a similar manner. Using a test function $\tilde{\phi}(x,y,z) := \tilde{\phi}(x) \in W^{1,\infty}(\Omega)\cap H_0^1(\Omega)$ in equation (26) we obtain

$$\int\int\int_{\Omega^1} \underbrace{\frac{\exp(\tilde{u}_i^\epsilon - \eta_i z_i \tilde{V}^\epsilon)}{\big(1+\sum_j \exp(\tilde{u}_j^\epsilon - \eta_j z_j \tilde{V}^\epsilon)\big)^2}}_{=:\alpha_i(\tilde{u}^\epsilon,\tilde{V}^\epsilon)} \partial_x\tilde{u}_i^\epsilon\partial_x\tilde{\phi}\,dx\,dy\,dz = 0.$$

We know that $\tilde{u}^\epsilon$ and $\tilde{V}^\epsilon$ converge weakly in $H^1(\Omega)$ and therefore strongly in $L^2(\Omega)$ and hence point wise a.e. to u and V respectively. We can therefore conclude that $\alpha_i(\tilde{u}^\epsilon,\tilde{V}^\epsilon)$ converges point wise to $\alpha_i(u,V)$. We further know that $\alpha_i(\tilde{u}^\epsilon,\tilde{V}^\epsilon) \leqslant k_3$ is uniformly bounded

in ϵ therefore converges, with the dominated convergence theorem A.2, also strongly in $L^2(\Omega)$. We thus get

$$
\begin{aligned}
&\left| \iiint_{\Omega'} \left(\alpha_i(\tilde{u}^\epsilon, \tilde{V}^\epsilon)\partial_x \tilde{u}_i^\epsilon - \alpha_i(u^0, V^0)\partial_x u_i^0\right)\partial_x \tilde{\phi}\, dx\, dy\, dz \right| \\
\leqslant &\left| \iiint_{\Omega'} \alpha_i(\tilde{u}^\epsilon, \tilde{V}^\epsilon)\partial_x \tilde{u}_i^\epsilon - \alpha_i(\tilde{u}^\epsilon, \tilde{V}^\epsilon)\partial_x u_i^0 \right. \\
&\left. + \alpha_i(\tilde{u}^\epsilon, \tilde{V}^\epsilon)\partial_x u_i^0 - \alpha_i(u^0, V^0)\partial_x u_i^0\, dx\, dy\, dz \right| \cdot \|\partial_x \tilde{\phi}\|_{L^\infty(\Omega)} \\
= &\left| \iiint_{\Omega'} \alpha_i(\tilde{u}^\epsilon, \tilde{V}^\epsilon)(\partial_x \tilde{u}_i^\epsilon - \partial_x u_i^0) \right. \\
&\left. + \partial_x u_i^0(\alpha_i(\tilde{u}^\epsilon, \tilde{V}^\epsilon) - \alpha_i(u^0, V^0))\, dx\, dy\, dz \right| \cdot \|\partial_x \tilde{\phi}\|_{L^\infty(\Omega)} \\
\leqslant &\|\partial_x \tilde{\phi}\|_{L^\infty(\Omega)} \Big(\underbrace{\left|(\partial_x \tilde{u}_i^\epsilon - \partial_x u_i^0, \alpha_i(\tilde{u}^\epsilon, \tilde{V}^\epsilon))_{L^2(\Omega)}\right|}_{\to 0} \\
&+ \underbrace{\|\alpha_i(\tilde{u}^\epsilon, \tilde{V}^\epsilon) - \alpha_i(u^0, V^0)\|_{L^2(\Omega)}}_{\to 0} \|\partial_x u_i^0\|_{L^2(\Omega)} \Big).
\end{aligned}
$$

The former because $\tilde{u}_i^\epsilon$ converges weakly in $H^1(\Omega)$ and therefore $\partial_x \tilde{u}_i^\epsilon$ converges weakly in $L^2(\Omega)$. Therefore

$$
\begin{aligned}
0 &= \iiint_{\Omega'} \alpha_i(\tilde{u}^\epsilon, \tilde{V}^\epsilon)\partial_x \tilde{u}_i^\epsilon \partial_x \tilde{\phi}\, dx\, dy\, dz \\
&\to \iiint_{\Omega'} \alpha_i(u^0, V^0)\partial_x u_i^0 \partial_x \tilde{\phi}\, dx\, dy\, dz \quad \forall \tilde{\phi} \in W^{1,\infty}(\Omega) \cap H_0^1(\Omega)
\end{aligned}
$$

and since $W^{1,\infty}(\Omega)$ is dense in $H_0^1(\Omega)$ we conclude that

$$
0 = \int_{-L}^{L} \alpha_i(u^0, V^0)\partial_x u_i^0 \partial_x \tilde{\phi}\, dx \underbrace{\iint dy\, dz}_{a(x)} \quad \forall \tilde{\phi} \in H_0^1(\Omega).
$$

Going back to strong formulation we have the full one dimensional Nernst-Planck equation given by (again suppressing any index 0)

$$
\partial_x \left(a(x) D_i \frac{\exp(u_i - \eta_i z_i V)}{(1 + \sum_j \exp(u_j - \eta_j z_j V))^2} \partial_x u_i \right) = 0. \tag{29}
$$

Part II

ANALYSIS

The second part of this thesis will be mainly concerned with the analytic properties of the modified PNP-Model. We will work step by step towards an existence proof for the stationary problem, based on a fixed point equation and application of Schauder's theorem. This existence proof will be the main result of this part.

4

EXISTENCE PROOF

Following the motivation and introduction of our modified model we will now try to verify the existence of weak solutions $u_i \in H^1(\Omega) \cap L^\infty(\Omega)$ and $V \in H^1(\Omega) \cap L^\infty(\Omega)$, with Ω being a Lipschitz domain. The prove presented in the following chapter is based on the work of [6], again more interim steps are shown in addition and some points are derived in a more rigorous way. If we hope to succeed in this endeavor some sort of regularity assumptions have to be made. The following seem reasonable enough and shall be valid until the end of this chapter.

$$\begin{aligned} &(A) \quad f \in L^\infty(\Omega),\ W_i^0 \in L^\infty(\Omega) \cap H^1(\Omega) \\ &(B) \quad V_D \in H^{\frac{1}{2}}(\Gamma_E) \cap L^\infty(\Gamma_E),\ u_i^D \in H^{\frac{1}{2}}(\Gamma_B) \cap L^\infty(\Gamma_B) \end{aligned}$$

The general idea for this prove is to construct a fixed point equation and then apply Schauder's theorem A.3 on

$$\mathcal{M} = \{(u_1, \dots, u_M) \in L^2(\Omega)^M \ \big|\ a \leqslant u_i \leqslant b \text{ a.e. } \}$$

with

$$a = \min_i \inf_{x \in \Gamma_B} u_i^D(x), \qquad b = \max_i \sup_{x \in \Gamma_B} u_i^D(x).$$

W.l.o.g. we set $\eta_i = 1$ throughout this section, but the results are true for arbitrary η_i. The corresponding fixpoint operator $\mathcal{F}$ will be split and discussed in two parts $\mathcal{F} = \mathcal{F}_2 \circ \mathcal{F}_1$, where $\mathcal{F}_1$ is defined by

$$\begin{aligned} \mathcal{F}_1 : \ & L^2(\Omega)^M \to L^2(\Omega)^M \times H^1(\Omega) \\ & (u_1, \dots, u_M) \mapsto (u_1, \dots, u_M, V) \end{aligned}$$

where V is the unique solution (cf. step 3) of

$$-\lambda^2 \Delta V = \sum_k z_k \frac{\exp(u_k - z_k V - W_k^0)}{1 + \sum_j \exp(u_j - z_j V - W_j^0)} + f \tag{30}$$

with boundary conditions (13) and (14). $\mathcal{F}_2$ is defined by

$$\begin{aligned} \mathcal{F}_2 : \ & \mathcal{F}_1(L^2(\Omega)^M) \subset L^2(\Omega)^M \times H^1(\Omega) \to L^2(\Omega)^M \\ & (u_1, \dots, u_M, V) \mapsto (v_1, \dots, v_M) \end{aligned}$$

where v_i are the unique weak solutions to the linear equations

$$\nabla \cdot \left(D_i \frac{\exp(u_i - z_i V - W_i^0)}{(1 + \sum_j \exp(u_j - z_j V - W_j^0))^2} \nabla v_i \right) = 0, \quad i = 1 \dots M$$

with boundary conditions

$$v_i = u_i^D \quad x \in \Gamma_B \quad \text{and} \quad \frac{\partial v_i}{\partial n} = 0 \quad x \in \partial\Omega \backslash \Gamma_B. \tag{31}$$

To use Schauder's Theorem we first need to verify certain properties of $\mathcal{M}$ and $\mathcal{F}$. We will do this in a step by step manor.

STEP 1: $\mathcal{M}$ is convex
It is very basic to see that for any $u, v \in L^2(\Omega)$ with $a \leqslant u, v \leqslant b$ also $w := \lambda u + (1-\lambda)v$, with $\lambda \in [0,1]$, is in $L^2(\Omega)$ and $a \leqslant w \leqslant b$.

STEP 2: $\mathcal{M}$ is closed
Moreover it is obvious that for any convergent sequence in $\mathcal{M}$ the limit is also in $\mathcal{M}$ and therefore $\mathcal{M}$ is closed.

STEP 3: $\mathcal{F}_1$ is well defined
First we will show that the functional

$$J(V) = \int_\Omega \frac{\lambda^2}{2}|\nabla V|^2 + \log\left(1 + \sum_j \exp(u_j - z_j V - W_j^0)\right) - fV \, dx \tag{32}$$

has a unique minimizer in

$$\begin{aligned} \mathcal{N} = \{V \in H^1(\Omega) \quad | \quad & V(x) = V_D(x) \quad \forall x \in \Gamma_E, \\ & \nabla V(x) \cdot n = 0 \quad \forall x \in \partial\Omega \backslash \Gamma_E\} \end{aligned} \tag{33}$$

and then that said unique minimizer is also a unique solution to (30),(13) and (14). To prove the former we want to use theorem A.5 and therefore need coercivity A.4 and uniform convexity of $J(V)$ in ∇V.

Using Young's inequality A.6 and Poincaré's inequality A.7 we derive

$$\begin{aligned} J(V) &\geqslant \frac{\lambda^2}{2}\|\nabla V\|^2_{L^2(\Omega)} - \int_\Omega fV \, dx \\ &\geqslant \frac{\lambda^2}{2}\|\nabla V\|^2_{L^2(\Omega)} - \frac{\epsilon}{2}\int_\Omega f^2 \, dx - \frac{1}{2\epsilon}\int_\Omega V^2 \, dx \\ &= \frac{\lambda^2}{2}\|\nabla V\|^2_{L^2(\Omega)} - \frac{\epsilon}{2}\int_\Omega f^2 \, dx - \frac{1}{2\epsilon}\|V\|^2_{L^2(\Omega)} \\ &\geqslant \frac{\lambda^2}{2}\|\nabla V\|^2_{L^2(\Omega)} - \frac{\epsilon}{2}\int_\Omega f^2 \, dx - \frac{1}{2\epsilon}C_F^2\left(\|\nabla V\|^2_{L^2(\Omega)} + \|V_D\|^2_{H^{\frac{1}{2}}(\Omega)}\right) \\ &= \left(\frac{\lambda^2}{2} - \frac{C_F^2}{2\epsilon}\right)\|\nabla V\|^2_{L^2(\Omega)} - \frac{\epsilon}{2}\int_\Omega f^2 \, dx - \frac{C_F^2}{2\epsilon}\|V_D\|_{H^{\frac{1}{2}}(\Omega)}. \end{aligned}$$

Now choosing ϵ in order that $\left(\frac{\lambda^2}{2} - \frac{C_F^2}{2\epsilon}\right) > 0$ we get coercivity for $J(V)$ with $a := \left(\frac{\lambda^2}{2} - \frac{C_F^2}{2\epsilon}\right)$ and $\beta := \frac{\epsilon}{2}\int_\Omega f^2 \, dx + \frac{C_F^2}{2\epsilon}\|V_D\|_{H^{\frac{1}{2}}(\Omega)}$.

We obtain convexity in p of $j(V,p) := \frac{\lambda^2}{2}|p|^2 + \log(1+\sum_j \exp(u_j - z_j V - W_j^0)) - fV$ by looking at the Hessian Matrix. It is easy to see that

$$\frac{\partial^2 j(V,p)}{\partial p_i p_j} = 0 \quad \forall i \neq j \qquad \text{and} \qquad \frac{\partial^2 j(V,p)}{\partial p_i^2} = \lambda^2 > 0$$

which makes the Hessian Matrix positive definite and therefore $j(V,p)$ uniformly convex in p. With theorem A.5 we now get a unique minimizer for (32) in (33).

Finally we show that this unique minimizer is also the unique solution of $\mathcal{F}_1$ by looking at the first variation of $J(V)$ that by definition is zero in any direction $\xi \in H^1_{0,\Gamma_E}(\Omega) := \{\xi \in H^1(\Omega) \mid \xi(x) = 0 \quad \forall x \in \Gamma_E\}$ if and only if V is said unique minimizer. Therefore

$$\begin{aligned} 0 &= \delta J(V,\xi) \\ &= \lambda^2 \int_\Omega \nabla V \nabla \xi \, dx - \int_\Omega \frac{\sum_k z_k \exp(u_k - z_k V - W_k^0)}{1+\sum_j \exp(u_j - z_j V - W_j^0)} \xi \, dx - \int_\Omega f\xi \, dx, \end{aligned}$$

which is exactly the weak formulation of (30), (13) and (14).

STEP 4: V is bounded in $H^1(\Omega)$ and $L^\infty(\Omega)$ independent of u
To show this we will first introduce

$$\mathcal{R}(V,u) = \frac{\sum_k z_k \exp(u_k - z_k V - W_k^0)}{1+\sum_j \exp(u_j - z_j V - W_j^0)}$$

for easier notation. It is obvious that $\mathcal{R}(V,u)$ is bounded in L^∞, as

$$\|\mathcal{R}(V,u)\|_{L^\infty(\Omega)} \leqslant \sum_k |z_k| \cdot \| \underbrace{\frac{\exp(u_k - z_k V - W_k^0)}{1+\exp(u_k - z_k V - W_k^0)}}_{\leqslant 1} \|_{L^\infty(\Omega)} \leqslant \sum_k |z_k|$$

It also holds $\mathcal{R}(V,u) \geqslant R(\tilde{V},u)$ for $V < \tilde{V}$ for any $x \in \mathbb{R}^3$, which we will use in Step 5, because

$$\begin{aligned} &\frac{\partial \mathcal{R}(V,u)}{\partial V} \\ &= \frac{(-\sum_k z_k^2 e^{u_k - z_k V - W_k^0})(1+\sum_j e^{u_j - z_j V - W_j^0}) + (\sum_k z_k e^{u_k - z_k V - W_k^0})^2}{(1+\sum_j e^{u_j - z_j V - W_j^0})^2} \end{aligned}$$

and

$$(-\sum_k z_k^2 e^{u_k - z_k V - W_k^0})(1+\sum_j e^{u_j - z_j V - W_j^0}) + (\sum_k z_k e^{u_k - z_k V - W_k^0})^2 \leqslant 0$$

as

$$(\sum_k z_k e^{u_k - z_k V - W_k^0})^2 \leqslant (\sum_k z_k^2 e^{u_k - z_k V - W_i^0})(\sum_k e^{u_k - z_k V - W_i^0}).$$

We used Cauchy Schwarz for the last inequality A.9. From the weak formulation of (30) we know

$$\lambda^2 \int_\Omega \nabla V \nabla \xi \, dx = \int_\Omega \mathcal{R}(V,u)\xi \, dx + \int_\Omega f\xi \, dx.$$

Taking the test function $\xi := (V-M)^+$ where $(.)^+ = max(.,0)$ and M is any sufficiently large constant so that $\xi \in H^1_{0,\Gamma_E}(\Omega)$, i.e. $M \geqslant M_0 := \|V_D\|_{L^\infty(\Gamma_E)}$.

$$\lambda^2 \int_\Omega \nabla V \nabla (V-M)^+ \, dx = \int_\Omega \mathcal{R}(V,u)(V-M)^+ \, dx + \int_\Omega f(V-M)^+ \, dx$$
$$\leqslant (\|f\|_{L^\infty(\Omega)} + \sum_k |z_k|) \int_\Omega (V-M)^+ \, dx.$$

From the Stampacchia theorem A.12 we know $\int_\Omega \nabla V \nabla (V-M)^+ \, dx = \int_\Omega (\nabla (V-M)^+)^2 \, dx$ and therefore for some constant C_1

$$\int_\Omega (\nabla (V-M)^+)^2 \, dx \leqslant C_1 \int_\Omega (V-M)^+ \, dx$$
$$\leqslant C_1 \|(V-M)^+\|_{L^p(\Omega)} meas(V > M)^{\frac{1}{q}}.$$

The last inequality is done by employing Hölder's inequality A.8 and p, q fulfilling the condition $\frac{1}{p} + \frac{1}{q} = 1$. From Kondrachov's embedding theorem A.11, Poincare's inequality A.7 and again Hölder's inequality we obtain

$$\|(V-M)^+\|^2_{L^p(\Omega)} \leqslant C_2 \|(V-M)^+\|^2_{H^1(\Omega)} \leqslant C_3 \|\nabla (V-M)^+\|^2_{L^2(\Omega)}$$
$$\leqslant C_4 \|(V-M)^+\|_{L^p(\Omega)} meas(V > M)^{\frac{1}{q}}$$

for some other constants C_2, C_3 and C_4, or after canceling $\|(V-M)^+\|_{L^p(\Omega)}$

$$\|(V-M)^+\|_{L^p(\Omega)} \leqslant C_4 meas(V > M)^{\frac{1}{q}}. \tag{34}$$

We also know that for any constant $H > M$

$$\|(V-M)^+\|^p_{L^p(\Omega)} = \int\limits_{(V>M)} ((V-M)^+)^p \, d \geqslant x \int\limits_{(V>H)} ((V-M)^+)^p \, dx$$
$$\geqslant \int\limits_{(V>H)} (H-M)^p \, dx = (H-M)^p \cdot meas(V > H).$$

Applied to (34) this yields

$$meas(V > H) \leqslant \frac{C_4^p}{(H-M)^p} meas(V > M) \quad \forall H > M \geqslant M_0$$

Now using the Lemma of Stampacchia A.13 we get that there is a H_0 so that for any $H > H_0$ we have $meas(V > H) = 0$ or in other words $\|V\|_{L^\infty(\Omega)} \leqslant H$ independent of u

Furthermore using Poincaré's inequality A.7 yields

$$\begin{aligned}\|V\|^2_{H^1(\Omega)} &= \|V\|^2_{L^2(\Omega)} + \|\nabla V\|^2_{L^2(\Omega)} \\ &\leqslant C_F^2(\|\nabla V\|_{L^2(\Omega)} + \|V_D\|_{H^{\frac{1}{2}}(\Gamma_D)})^2 + \|\nabla V\|^2_{L^2(\Omega)} \\ &\leqslant 2C_F^2(\|\nabla V\|^2_{L^2(\Omega)} + \|V_D\|^2_{H^{\frac{1}{2}}(\Gamma_D)}) + \|\nabla V\|^2_{L^2(\Omega)} \\ &\leqslant \tilde{C}(\|\nabla V\|^2_{L^2(\Omega)} + \|V_D\|^2_{H^{\frac{1}{2}}(\Gamma_D)})\end{aligned}$$

and using (32) provides

$$\begin{aligned}\|V\|^2_{H^1(\Omega)} &\leqslant \tilde{C}\frac{2}{\lambda^2}J(V) + \tilde{C}\|V_D\|^2_{H^{\frac{1}{2}}(\Gamma_D)} \\ &\leqslant \tilde{C}\frac{2}{\lambda^2}J(\tilde{V}) + \tilde{C}\|V_D\|^2_{H^{\frac{1}{2}}(\Gamma_D)} \\ &\leqslant \tilde{C}\frac{2}{\lambda^2}\tilde{J}(\tilde{V}) + \tilde{C}\|V_D\|^2_{H^{\frac{1}{2}}(\Gamma_D)}\end{aligned}$$

where $\tilde{V}$ is an arbitrary element of $\mathcal{N}$ and $\tilde{J}$ being defined as

$$\tilde{J}(V) = \int_\Omega \frac{\lambda^2}{2}|\nabla V|^2 + \log\left(1 + \sum_j \exp(b_j - z_j V - W_j^0)\right) - fV\,dx.$$

V is therefore bounded in H^1 independently of u.

STEP 5: F_1 is continuous

F_1 is even Lipschitz continuous. For 2 weak solutions V and $\tilde{V}$ corresponding to u and $\tilde{u}$ we subtract the weak formulations

$$\begin{aligned}\int_\Omega \lambda^2\nabla(V-\tilde{V})\nabla\phi\,dx &= \int_\Omega (\mathcal{R}(V,u) - \mathcal{R}(\tilde{V},\tilde{u}))\phi\,dx \\ &= \int_\Omega (\mathcal{R}(\tilde{V},u) - \mathcal{R}(\tilde{V},\tilde{u}))\phi\,dx + \int_\Omega (\mathcal{R}(V,u) - \mathcal{R}(\tilde{V},u))\phi\,dx\end{aligned}$$

Now using the test function $\phi := V - \tilde{V}$, the monotony of $\mathcal{R}$ in V and again Cauchy Schwarz A.9 we obtain

$$\begin{aligned}\lambda^2\|\nabla(V-\tilde{V})\|^2_{L^2(\Omega)} &= \int_\Omega (\mathcal{R}(\tilde{V},u) - \mathcal{R}(\tilde{V},\tilde{u})(V-\tilde{V})\,dx \\ &\quad + \int_\Omega \underbrace{(\mathcal{R}(V,u) - \mathcal{R}(\tilde{V},u)(V-\tilde{V})}_{\leqslant 0}\,dx \\ &\leqslant \|V-\tilde{V}\|_{L^2(\Omega)}\|\mathcal{R}(\tilde{V},u) - \mathcal{R}(\tilde{V},\tilde{u})\|_{L^2(\Omega)}.\end{aligned}$$

V and $\tilde{V}$ satisfy the same boundary conditions therefore $V - \tilde{V} \in H^1_0(\Omega)$ and we can use Poincare's inequality A.7 to gain

$$\|V-\tilde{V}\|_{H^1(\Omega)} \leqslant C\|\nabla(V-\tilde{V})\|_{L^2(\Omega)}$$

for some constant C. Therefore altogether

$$\|V-\tilde{V}\|_{H^1(\Omega)} \leqslant \frac{C}{\lambda^2}\|\mathcal{R}(\tilde{V},u) - \mathcal{R}(\tilde{V},\tilde{u})\|_{L^2(\Omega)}$$

We know that and $\mathcal{R}$ is differentiable in u and the derivative is bounded, as $u, \tilde{u}, V$ and $\tilde{V}$ are bounded. Therefore R is Lipschitz continuous in u and

$$\|V - \tilde{V}\|_{H^1(\Omega)} \leqslant \frac{\tilde{C}}{\lambda^2} \|u - \tilde{u}\|_{L^2(\Omega)}$$

holds.

STEP 6: $\mathcal{F}_2$ is well defined on $\mathcal{F}_1(\mathcal{M})$
The standard theory for elliptic equations [19, 20] implies the existence and uniqueness of a weak solution $v_i \in H^1(\Omega)$ to

$$\nabla \cdot (A_i \nabla v_i) = 0 \qquad \text{in } \Omega$$

with boundary conditions (31) and

$$A_i := D_i \frac{\exp(u_i - z_i V - W_i^0)}{(1 + \sum_j \exp(u_j - z_j V - W_j^0))^2},$$

as

$$0 < D_i \frac{e^{a - |z_i| \|V\|_{L^\infty(\Omega)} - \|W_i^0\|_{L^\infty(\Omega)}}}{\left(1 + \sum_j e^{b - |z_j| \|V\|_{L^\infty(\Omega)} - \|W_j^0\|_{L^\infty(\Omega)}}\right)^2} \leqslant A_i \leqslant D_i. \tag{35}$$

Now we need to verify that $a \leqslant v_i \leqslant b$ still holds true. To do that we take a test function $\xi := (v_i - b_i)^+$ and have for our weak formulation

$$\int_\Omega A_i \nabla v_i \nabla (v_i - b_i)^+ \, dx = 0.$$

With (35), the theorem of Stampacchia A.12 and Poincare's Inequality A.7 we can show

$$\begin{aligned} 0 &= \int_\Omega A_i \nabla v_i \nabla (v_i - b_i)^+ \, dx \geqslant C_6 \int_\Omega \nabla v_i \nabla (v_i - b_i)^+ \, dx \\ &= C_6 \int_\Omega (\nabla (v_i - b_i)^+)^2 \, dx \geqslant C_7 \int_\Omega ((v_i - b_i)^+)^2 \, dx \geqslant 0 \end{aligned}$$

for some constants C_6, C_7. We therefore know $\text{meas}(v_i > b_i) = 0$ and repeating the above trick with the test function $\xi := (v_i - a_i)^- := (-(v_i - a_i))^+$ also $\text{meas}(v_i < a_i) = 0$.

From Relich-Kondrachov's embedding theorem A.11 we know that the embedding $H^1(\Omega) \hookrightarrow L^2(\Omega)$ is compact and therefore that $\mathcal{F}_2(\mathcal{F}_1(\mathcal{M}))$ is precompact and part of $\mathcal{M}$. Which gives us

STEP 7: $\mathcal{F}_2(\mathcal{F}_1(\mathcal{M})) \in \mathcal{M}$ is precompact in $L^2(\Omega)$
Note that any fixed point $u_i \in L^2(\Omega)$ of $\mathcal{F}_2 \circ \mathcal{F}_1(\mathcal{M})$ is therefore also in $H^1(\Omega)$

STEP 8: $\mathcal{F}_2$ is continuous
Consider the sequences $V^k \to V$ in $H^1(\Omega)$ and $u_i^k \to u_i$ in $L^2(\Omega)$, then A_i^k is bounded uniformly in k as in (35) and therefore again with the dominated convergence theorem A.2 $A_i^k \to A_i$ in $L^2(\Omega)$. Let now v_i^k be the unique weak solutions to

$$\nabla(A_i^k \nabla v_i^k) = 0$$

and the given boundary conditions. As A_i^k is bounded and all v_i^k fulfill the same boundary conditions we know from the standard theory of elliptic PDEs [20] that v_i^k is bounded in $H^1(\Omega)$ uniformly in k. With the theorem of Eberlein-Šmulian A.1 we have weak convergence $v_i^{kl} \rightharpoonup v_i$ in $H^1(\Omega)$ along a subsequence. This however implies strong and weak convergence of $v_i^{kl} \rightharpoonup v_i$ in $L^2(\Omega)$ and also more importantly weak convergence of $\nabla v_i^{kl} \rightharpoonup \nabla v_i$ in $L^2(\Omega)$. Now for any test function $\phi \in W^{1,\infty}(\Omega) \cap H_0^1(\Omega)$

$$\begin{aligned}
&\left| \int_\Omega (A_i^{kl} \nabla v_i^{kl} - A_i \nabla v_i) \nabla \phi \, dx \right| \\
&\qquad = \left| \int_\Omega (A_i^{kl} \nabla v_i^{kl} - A_i \nabla v_i^{kl} + A_i \nabla v_i^{kl} - A_i \nabla v_i) \nabla \phi \, dx \right| \\
&\qquad \leqslant \|\nabla \phi\|_{L^\infty(\Omega)} \int_\Omega \left| (A_i^{kl} - A_i) \nabla v_i^{kl} - A_i (\nabla v_i^{kl} - \nabla v_i) \right| dx \\
&\qquad \leqslant \|\nabla \phi\|_{L^\infty(\Omega)} \Bigg(\underbrace{\|A_i^{kl} - A_i\|_{L^2(\Omega)}}_{\to 0} \underbrace{\|\nabla v_i^{kl}\|_{L^2(\Omega)}}_{\leqslant C} \\
&\qquad\quad + \underbrace{\left| \left(\nabla v_i^{kl} - \nabla v_i, A_i \right)_{L^2(\Omega)} \right|}_{\to 0} \Bigg).
\end{aligned}$$

Therefore

$$0 = \int_\Omega A_i^{kl} \nabla v_i^{kl} \nabla \phi \to \int_\Omega A_i \nabla v_i \nabla \phi \, dx \qquad \forall \phi \in W^{1,\infty}(\Omega) \cap H_0^1(\Omega)$$

and since $W^{1,\infty}(\Omega)$ is dense in $H_0^1(\Omega)$ we can conclude that

$$0 = \int_\Omega A_i \nabla v_i \nabla \phi \, dx \qquad \forall \phi \in H_0^1(\Omega).$$

Because of the linearity and continuity of he trace operator we know that it is weak sequentially continuous and therefore that v_i fulfills the boundary conditions (31). Because of the uniqueness of this solution we can use A.10 to show that not only $v_i^{kl} \to v_i$ in $L^2(\Omega)$ but also $v_i^k \to v_i$ in $L^2(\Omega)$.

STEP 9: Application of Schauder's theorem
We can now use Schauder's fixed point theorem A.3 to show the existence of a fixed point $u \in \mathcal{M}$ of $\mathcal{F}_2 \circ \mathcal{F}_1(\mathcal{M})$.

STEP 10: By transforming back into our original variables $c_i$we get the following result

Theorem 4.1 (Global Existence)**:** *Let $\Omega \subset \mathbb{R}^n$ be an open Lipschitz domain and assumptions (A) and (B) be satisfied, then there exists a weak solution*

$$(V, u_1, \dots, u_n) \in H^1(\Omega)^{M+1} \cap L^\infty(\Omega)^{M+1}$$

of our problem

$$-\lambda^2 \Delta V = \sum_k z_k \frac{\exp(u_k - z_k V - W_k^0)}{1 + \sum_j \exp(u_j - z_j V - W_j^0)} + f \tag{36}$$

$$\nabla \cdot \left(D_i \frac{\exp(u_i - z_i V - W_i^0)}{(1 + \sum_j \exp(u_j - z_j V - W_j^0))^2} \nabla u_i \right) = 0, \quad i = 1 \dots M \tag{37}$$

with boundary conditions (31), (13) and (14).

Part III

NUMERICS

In this part we will describe our approach of an implementation of the one dimensionalised nonlinear Poisson-Nernst-Planck Equations, as well as comparisons to other results and numerical tests as to why our implementation makes sense. In the end a small outlook will be given on future areas of investigations and applications.

5 NUMERICAL IMPLEMENTATION

In this chapter we want to present a simple implementation for the system of one dimensional equations established in chapter 3.2

$$\partial_x\big(a(x)D_i\frac{\exp(u_i-\eta_i z_i V)}{(1+\sum_j \exp(u_j-\eta_j z_j V))^2}\partial_x u_i\big)=0 \tag{38}$$

$$-\lambda^2\partial_x\big(a(x)\partial_x V(x)\big)=a(x)\big(\frac{\sum_k z_k\exp(u_k-\eta_k z_k V)}{1+\sum_j \exp(u_j-\eta_j z_j V)}+f(x)\big). \tag{39}$$

in $\Omega=[0,1]$ and boundary conditions $u_i(0)=u_i^D(0)$, $u_i(1)=u_i^D(1)$, $V(0)=V^D(0)$ and$V(1)=V^D(1)$, where

$$u_i^D := \log c_i^D - \log\big(1-\sum_j c_j^D\big)+\eta_i z_i V^D \quad x\in\{0,1\}.$$

5.1 FURTHER MODEL ASSUMPTIONS

We remember the assumptions made in chapter 3.1, see also figure 2. The length and radius of our cylinder are $r_c = 0.4$ nm and $l_c = 1$ nm. The length and outer radius of our 2 baths are $l_b = 2$ nm and $r_b = 2.4$ nm respectively. This makes for a total length of $\tilde{L} = 5\,nm$ for our model. For the dimension of the particles we assume particle radius of 0.15 nm for all particles and according to that a typical maximal concentration of 61.5 mol/l [6] or $3.7037\cdot 10^{25}$ N/l where N denotes the number of particles. In Table 1 we outline the most important physical constants used for our simulations.

Our typical properties for scaling will be $\tilde{L} = 5\,nm$ for length and $\tilde{V} = 100\,V$ for voltage and we also assume $\mu_i = \frac{1}{k_B T}$ [7] and a temperature of 300 K. This obviously gives

$$\lambda^2=\frac{\epsilon_0\epsilon_r\tilde{V}}{e\tilde{L}^2\tilde{c}}=4.68\times10^{-4} \qquad \text{and} \qquad \eta=\frac{e\tilde{V}}{k_B T}=3.87.$$

To summarize see table 2. In the baths we assume 3 species Ca^{2+}, Na^{+} and Cl^{-} their concentration given by c_1, c_2, c_3 or their transformed concentration u_1, u_2, u_3, as well as a stationary species $O^{-\frac{1}{2}}$ (describing a O_2^- molecule) that only resides inside the channel given by $c_{O^{-1/2}}$. This concentration is assumed to be known and therefore does not have to be transformed into entropy variables. It in fact cannot even be transformed as it is 0 on the boarder. This slightly changes the equations calculated in chapter 3.1 into

Meaning	Value	Unit
Boltzmann constant k_B	$1.3806504 \times 10^{-23}$	J/K
Avogadros constant	$6.02214179 \times 10^{23}$	N/mol
Vacuum permittivity ϵ_0	$8.854187817 \times 10^{-12}$	F/m
Relative permittivity ϵ_r	78.4	
Elementary charge e	1.602176×10^{-19}	C
Particle Radius	0.15	nm
Ion charge Ca^{2+} z_1	2	
Ion charge Na^{+} z_2	1	
Ion charge Cl^{-} z_3	-1	
Ion charge $O^{-\frac{1}{2}}$ z_O	$-\frac{1}{2}$	

Table 1: Physical parameters cf. [7]

Meaning	Value	Unit
Scaling length $\tilde{L}$	5	nm
Scaling voltage $\tilde{V}$	100	V
Temperature T	300	K
λ^2	4.68×10^{-4}	
η	3.87	

Table 2: Model assumptions cf. [7]

$$0 = \partial_x\big(a(x)D_i\frac{\exp(u_i-\eta_i z_i V)(1-c_{O^{-1/2}})^2}{(1+\sum_j \exp(u_j-\eta_j z_j V))^2}\partial_x u_i\big) \tag{40}$$

$$\begin{aligned}&-\lambda^2\,\partial_x\big(a(x)\partial_x V(x)\big)\\ &\quad= a(x)\Big(\sum_k z_k\frac{\exp(u_k-\eta_k z_k V)(1-c_{O^{-1/2}})^2}{1+\sum_j \exp(u_j-\eta_j z_j V)}+f(x)\Big).\end{aligned} \tag{41}$$

This can be easily verified by applying the transformation to entropy variables done in chapter 2.4 onto all but one concentration variable $c_{O^{-1/2}}$. The permanent charge density in our model is given by $f(x) = z_O \cdot c_{O^{-1/2}}(x)$ and the area function $a(x)$ gives the scaled area of the cross section of our geometry, cf. figure 2.

5.2 SOLVING METHOD

We solve (40) and (41) in an iterative manner, comparable to the way the fixed point iteration in the existence proof worked.

STEP 1: Given some Value V and v_i we solve a linearized equation

$$0 = \partial_x\left(a(x)D_i\frac{\exp(v_i - \eta_i z_i V)(1 - c_{O^{-1/2}})^2}{(1 + \sum_j \exp(v_j - \eta_j z_j V))^2}\partial_x u_i\right)$$

using standard 1D FEM [1] discretization on some mesh $M := \{x_1, \ldots, x_N\}$.

STEP 2: We use the resulting u_i to calculate a new solution for V out of (41) using Newton iteration to solve the non linear system of equations resulting from using standard FDM [1] on M.

STEP 3: Goto Step 1 until convergence.

6 RESULTS, TESTS AND OUTLOOK

In this chapter several results and tests of the method introduced in chapter 5 will be outlined as well as compared to other results from literature. All calculations were done in Matlab R2015b on a MacBook Air 13-inch Mid 2012 Edition.

6.1 SAMPLE CALCULATION

Our boundary conditions are chosen according to [8]. For the unscaled and untransformed numbers cf. table 3.

Quantity/Species	Variable	Value
Concentration Ca^{2+}	$\tilde{u}_1^D(0)$	5×10^{-3} mol/l
	$\tilde{u}_1^D(1)$	10^{-1} mol/l
Concentration Na^{+}	$\tilde{u}_2^D(0)$	10^{-1} mol/l
	$\tilde{u}_2^D(1)$	10^{-1} mol/l
Concentration Cl^{-}	$\tilde{u}_3^D(0)$	1.1×10^{-1} mol/l
	$\tilde{u}_3^D(1)$	3×10^{-1} mol/l
Potential	$\tilde{V}^D(0)$	5×10^{-2} V
	$\tilde{V}^D(1)$	0 V

Table 3: Unscaled and untransformed boundary conditions

Our oxygen concentration will have a maximum concentration of 55 mol/l in the channel and 0 mol/l outside. For the transition we investigated several options ranging from a non continuous step transition, linear interpolation to smoother interpolations with very similar results. In figure 3 you can see as an example the unscaled oxygen concentration with linear interpolation.

The resulting concentration profiles for the Calzium, Sodium and Chloride ions as well as the potential profile can be seen in figure 4 and 5 respectively. The profiles are in excellent agreement with the results given in [6] and [7]. What's more important is the desired effect of the modified PNP-Model to prevent overcrowding inside the channel which can clearly be seen in figure 6 and which generally is not the case in the standard linear PNP-Model [6]. The crowding effects leads to a significant reduction in ion concentration inside the channel compared to similar linear results in [6]. The channel is also ion selective. In figure 4 we can see that for chloride $c_3 = 0$ and also $\partial_x c_3 = 0$ inside the channel which results in the flow of chloride, cf.

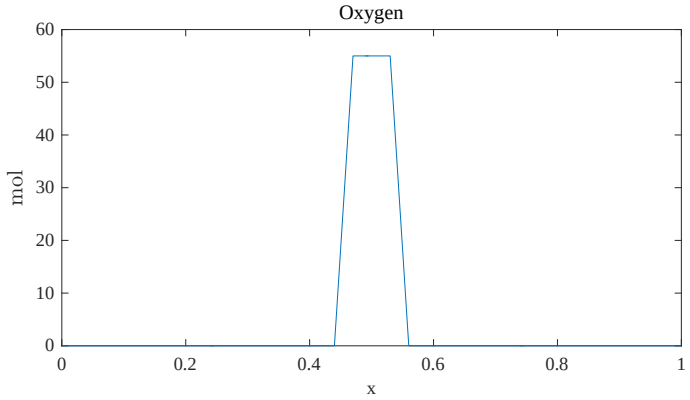

Figure 3: Oxygen profile with linear interpolation

(9), being zero. For now the ion selectivity in our model is solely dependent on the charge and not the radii of the ion. It would however be fairly simple to adapt it to differently sized particles, cf. 6.3.

6.2 SEVERAL TESTS

To further make our results plausible, we conducted a series of common numerical tests. The first one was a numerical convergence test, the second one a residual error test and for the last one we looked at the peaks in figure 4, especially Ca^{2+} and Na^{+} and wanted to know whether they converge with increasing gradient in the oxygen profile.

6.2.1 *Numerical convergence test*

In a convergence test ideally what we would want to see is the calculated solutions converge to the exact solution with decreasing mesh size h in some kind of order $\mathcal{O}(h^{\alpha})$. Unfortunately that exact solution is almost never known so instead a numerical one is used with at least 4 times smaller mesh size than the smallest one you want to compare. In figure 7 you can see in a sample test with equidistant mesh that convergence occurs with $\alpha \approx 1.2$. For sufficiently smooth data one might expect $\mathcal{O}(h^2)$ [21]. This discrepancy is very likely caused by the mixture of the FEM- and FD-method described in chapter 5.2 and could probably be avoided by a full FEM implementation of both equations. Tests with different kinds of meshes or different kinds of model assumptions and boundary conditions all yielded similar results.

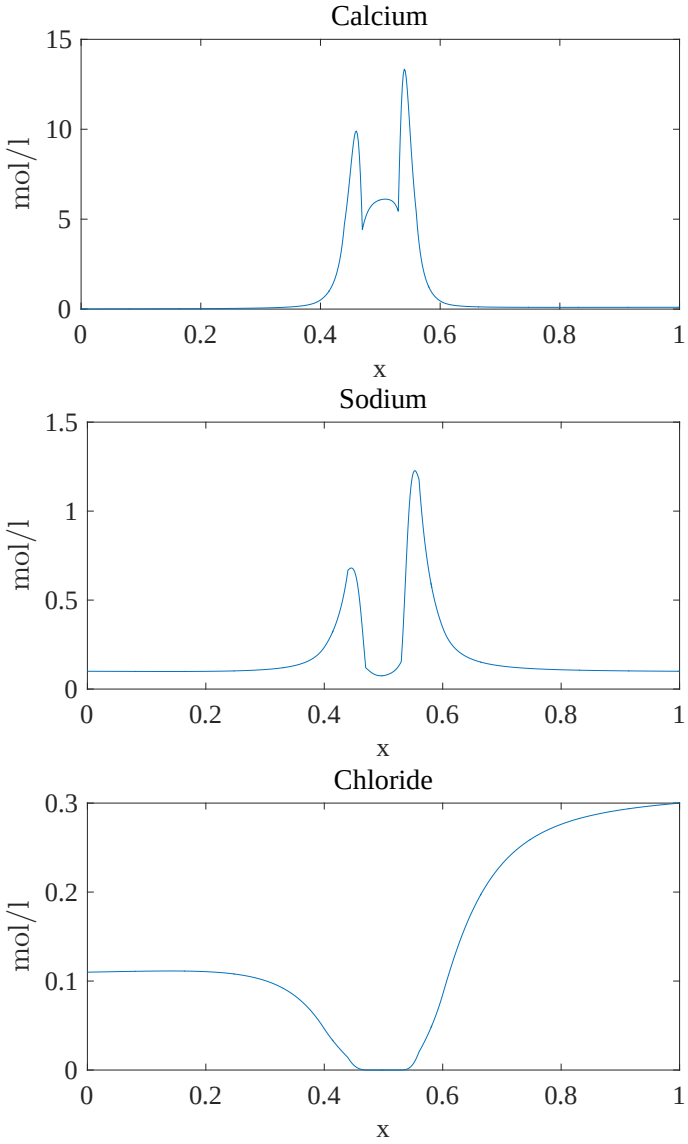

Figure 4: Unscaled concentration profiles

6.2.2 *Residual error test*

The idea of this test is to investigate the behavior of the Residuum, i.e. our numerical solution inserted into our original equations, with decreasing mesh size. E.g. for (40)

$$\mathcal{R}(u_i^N)w = \int_\Omega \underbrace{a(x)D_i \frac{\exp(u_i^N - \eta_i z_i V^N)(1 - c_{O^{-1/2}})^2}{(1 + \sum_j \exp(u_j^N - \eta_j z_j V^N))^2}}_{A_i(u^N)} \partial_x u_i^N \partial_x w \, dx$$

for $w \in H_0^1(\Omega)$ and u^N, V^N in the appropriate finite dimensional subspace $H_N \subset H^1(\Omega)$ according to some mesh. To evaluate $\|R(u^N)\|_{H^{1*}}$

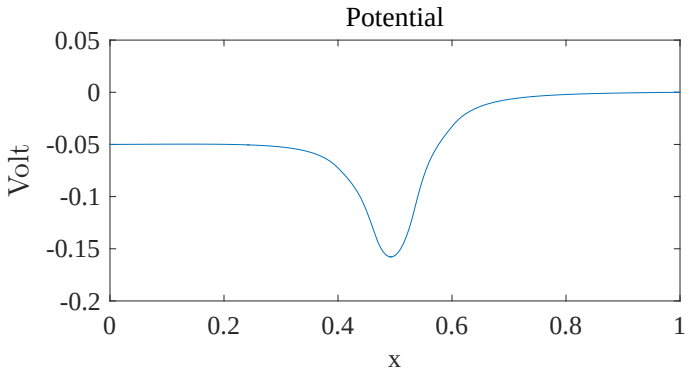

Figure 5: Unscaled potential profile

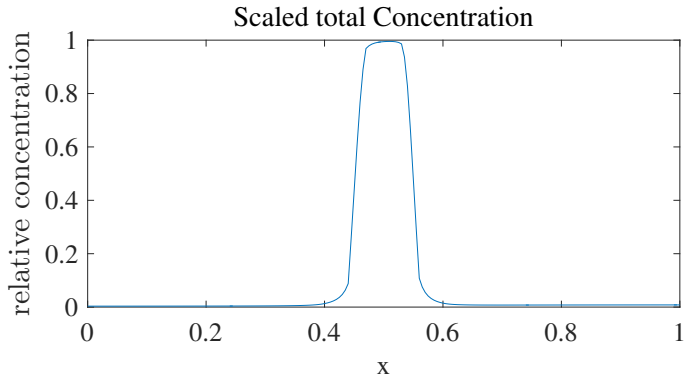

Figure 6: Crowding effects inside the channel

we used the estimation shown in [22] and adapted it to our problem, to get

$$\|R(u^N)\|_{H_0^{1*}} \leqslant C \sqrt{\sum_{T\in\mathcal{T}} h_T^2 \|R_T(u^N)\|_{L^2(T)} + \sum_{e\in\mathcal{E}^0} |R_e(u^N)|^2},$$

for some unknown C. With

$$\begin{aligned} R_T(u^N) &= \partial(A_i(u^N)\partial u^N)|_T \\ R_e(u^N) &= A_i(u^N(e))\Big(\partial_x u^N(e^+) - \partial_x u^N(e^-)\Big) \end{aligned}$$

and $\mathcal{T}$ being the set of elements and $\mathcal{E}^0$ being the set of inner nodes. As seen in figure 8, $\|R(u^N)\|_{H_0^{1*}} = \mathcal{O}(h^{\frac{1}{2}})$.

6.2.3 *Peak maximum*

The peaks on the outside of the channel in the calcium and sodium concentration, see figure 4, can, in a biological sense, very plausibly be explained by a congestion due to the volume exclusion inside the channel. To make sure it is not a relic of the numerical calculation

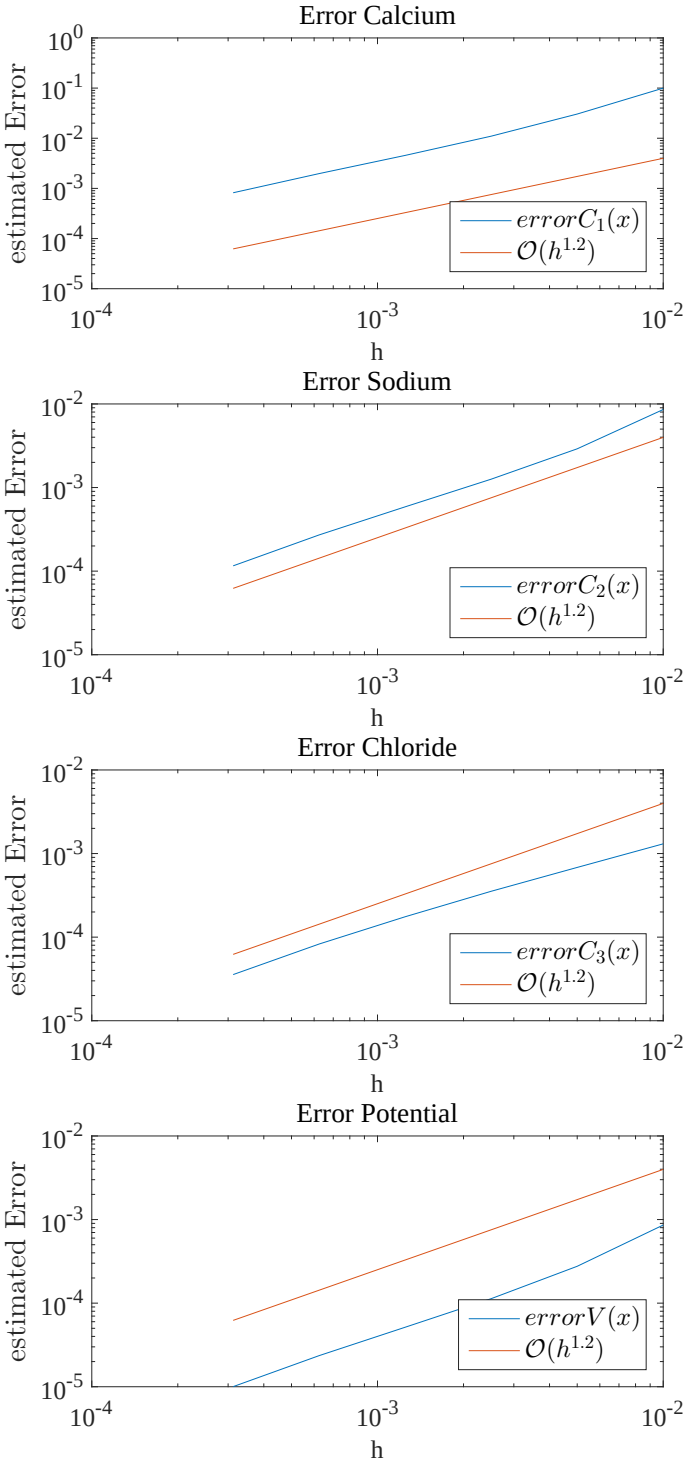

Figure 7: Estimated numerical errors

resulting from, for example, an amplification of the un-smoothness of the oxygen concentration in this area we wanted to investigate whether the peak grows with increasing gradient of the oxygen concentration. To do this we took an oxygen profile like in 9 and de-

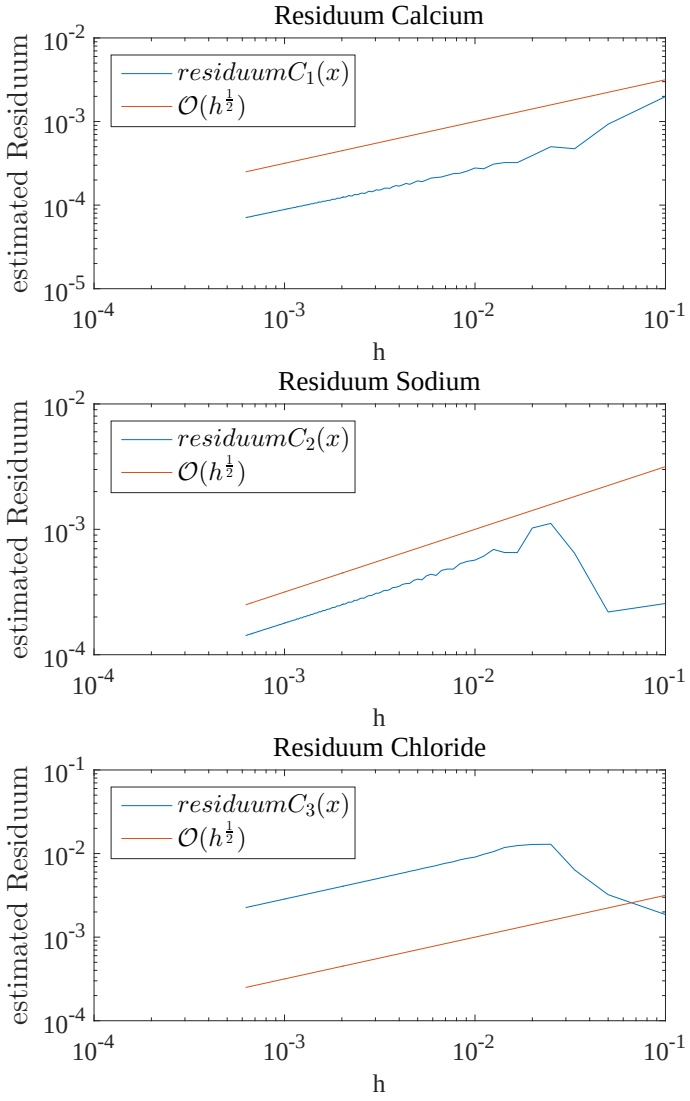

Figure 8: Estimated residuals

creased ϵ in every calculation. In Figures 11 and 12 you can see the results of such a test with element size $h \approx 10^{-3}$. Obviously the peak will not grow further if the grid can no longer distinguish between a piecewise linear 9 and a piecewise constant 10 Oxygen profile. Nevertheless it can be assumed that the peeks are indeed bounded by some value for even higher resolutions. The shrinking of the peak for very low gradient is a result of the simplicity of the test, as the plot does actually shows the max value of C, which for low gradients is not necessarily assumed at the entrance of the channel.

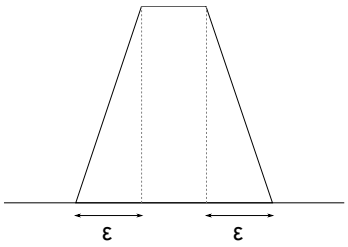

Figure 9: Sketch of piecewise linear oxygen profile

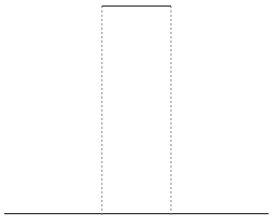

Figure 10: Sketch of piecewise constant oxygen profile

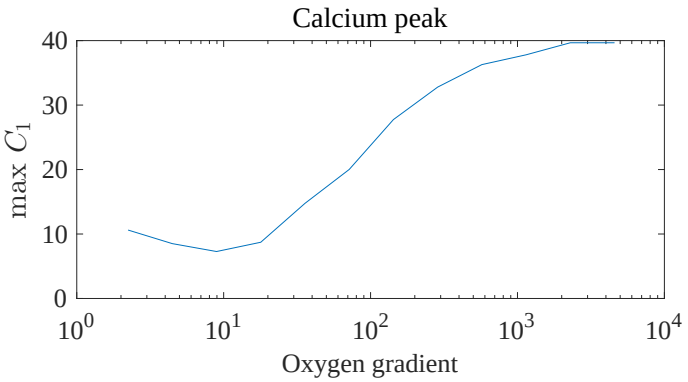

Figure 11: Semilogplot for peak size over the maximal gradient in the oxygen concentration in Ca^{2+}

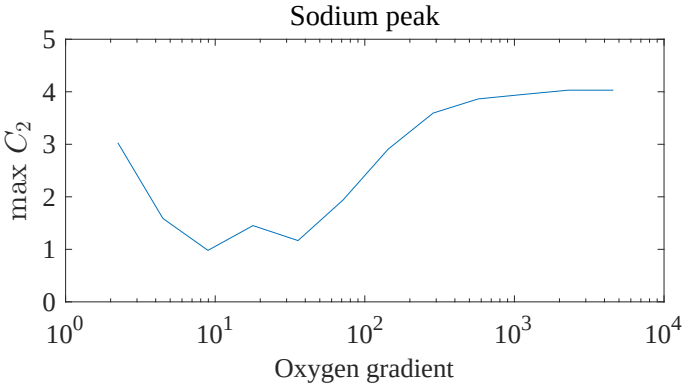

Figure 12: Semilogplot for peak size over the maximal gradient in the oxygen concentration in Na^{+}

6.3 SUMMARY AND OUTLOOK

The standard PNP-Model is one of the most common ways to describe ion transport through biological or synthetic channels. Its application in confined geometries is however highly questionable as the effects of volume exclusion are not taken into consideration. This effect becomes relevant if the channel dimensions become comparable to the ion size.

The nonlinear model investigated can describe these phenomena more realistically, as it detects crowding inside the channel and reduces the flow of ions in the channel accordingly. Furthermore it is able to represent the ion selectivity of the channels, as depending on the permanent charge density inside the channel some ions pass through more easily than others.

The existence proof from chapter 4 showcases that it is indeed possible to find solutions to said model and also indicates a way of implementing it.

The dimension reduction in chapter 3 is a fast and simple way to calculate our model and in our simulation chapter 5 we have shown a way to successfully implement this in Matlab. The tests and comparisons done in chapter 6 make our calculations plausible.

In the future it would be interesting to modify the implementation for different particle sizes and investigate the resulting selectivity of the ion channels. Another obvious way forward would be a 2D or even 3D implementation of the modified PNP-Model to be able to treat even more realistic cases.

Part IV

APPENDIX

A

THEOREMS AND DEFINITIONS

Theorem A.1 (Eberlein-Šmulian)**:** *A Banach Space is reflexive if and only if every bound sequence has a weak convergent subsequence.[23]*

Theorem A.2 (Lebesgue's Dominated Convergence Theorem)**:** *Let f_n be sequence of measurable functions on a measure space $\mathcal{M}(\Omega, \Sigma, \mu)$ converging a.e. to a function f and let g be a measurable function with $\int_\Omega |g|\,d\mu < \infty$ and $|f_n| \leqslant g|$ then f_n and f are integrable and*

$$\lim_n \int_\Omega f_n \, d\mu = \int_\Omega f \, d\mu.$$

[24]

Theorem A.3 (Schauder fixed point theorem)**:** *Let X be a Banach space and K a non empty convex subspace of X. Let further $F : K \to K$ be a continuous map. If either*

- *K is compact or*
- *K is closed and $F(K)$ is relative compact*

then F has at least one fixed point in K [25].

For the next theorem we first need the concept of coercivity

Definition A.4 (Coercivity)**:** *A functional $\mathcal{F}(u) = \int_\Omega F(x, u, p)\,dx$ with $p = \nabla u$ is called coercive if $\exists \alpha > 0,\ \beta > 0$ so that*

$$\mathcal{F}(u) \geqslant \alpha \|p\|^q_{L^q(\Omega)} - \beta.$$

Theorem A.5: *Let $U := \{u \in W^{1,q}(\Omega)|$ fullfilling (42) and (43)$\}$*

$$u(x) = g \quad \forall x \in \Gamma_D \subseteq \partial\Omega \quad g : \Gamma_D \to \mathbb{R} \tag{42}$$

$$\frac{\partial u}{\partial n} = 0 \quad \forall x \in \Gamma_N = \partial\Omega \backslash \Gamma_D \tag{43}$$

and let further be $\mathcal{F} : U \to \mathbb{R}$

$$\mathcal{F}(u) = \int_\Omega F(x, u, p)\,dx$$

If $\mathcal{F}$ further be coercive and F smooth and uniformly convex in p and $U \neq \{\}$ then there exists a unique minimizer of $\mathcal{F}$ in U.

Proof. The proof in [26] can be adapted to our modified boundary conditions, as the theorem of Mazur used in step 3 can still be applied to an accordingly modified $W^{1,q}_0(\Omega)$. □

Theorem A.6 (Young's inequality)**:** *For any real* a, b *and* $\epsilon > 0$

$$ab \leqslant \frac{a^2}{2\epsilon} + \frac{\epsilon b^2}{2}$$

Proof.

$$0 \leqslant (a\sqrt{\epsilon} - \frac{b}{\sqrt{\epsilon}})^2 = a^2\epsilon - 2ab + \frac{b^2}{\epsilon}$$
$$ab \leqslant \frac{a^2\epsilon}{2} + \frac{b^2}{2\epsilon}$$

□

Next we need two different forms of the Poincaré inequality.

Theorem A.7 (Poincaré inequality)**:**

- *Let* Ω *be a bounded domain*
  $\|v\|_{L^2(\Omega)} \leqslant C_1 \|\nabla v\|_{L^2(\Omega)} \quad \forall v \in H_0^1(\Omega)$ *[27].*
- *Let* Ω *also be a Lipschitz domain with* $\emptyset \neq \Gamma_D \subset \partial\Omega$
  $\|v\|_{L^2(\Omega)} \leqslant C_2 \left(\|\nabla v\|_{L^2(\Omega)} + \|v_D\|_{H^{\frac{1}{2}}(\Gamma_D)} \right)$ *[1].*

Theorem A.8 (Hölder's inequality)**:** *Let* p *and* q *with* $\frac{1}{p} + \frac{1}{q} = 1$ *or* $p = 1$ *and* $q = \infty$ *then*

$$\|fg\|_{L^1(\Omega)} \leqslant \|f\|_{L^p(\Omega)} \|g\|_{L^q(\Omega)}$$

[24].

A special case of the Hölder's inequality with $p = q = 2$ is the Cauchy-Schwarz inequality

Theorem A.9 (Cauchy-Schwarz inequality)**:**

$$\|fg\|_{L^1(\Omega)} \leqslant \|f\|_{L^2(\Omega)} \|g\|_{L^2(\Omega)}.$$

Theorem A.10: *Let* X *be a Banach space and* a_n *be a sequence in* X*. If for any subsequence* a_{n_k} *of* a_n *there exists a subsequence* $a_{n_{k_i}}$ *that converges against* $a \in X$ *then* a_n *also converges against* a*.*

Proof. Assume a_n does not converge against a. Then $\forall \epsilon > 0$, $\exists$ subsequence a_{n_k} with

$$\|a_{n_k} - a\|_X > \epsilon \quad \forall n_k$$

Therefore no subsequence of a_{n_k} converges to a. □

Theorem A.11 (Kondrachov embedding theorem)**:** *Let* Ω *be an open bounded Lipschitz domain and* $1 \leqslant p < n$ *then* $W^{1,p}(\Omega)$ *is compactly embedded in* $L^q(\Omega)$ *for each* $1 \leqslant q < p^*$ *and* $p^* := \frac{np}{n-p}$*[28].*

Theorem A.12 (Stampacchia)**:** *Let* $\Omega \subset \mathbb{R}^n (n \leqslant 1)$ *be a bounded,* $1 \leqslant p < \infty$ *and* $u \in W^{1,p}(\Omega)$*. Then* $u^+ = \max\{u, 0\} \in W^{1,p}(\Omega)$ *and*

$$\nabla u^+ = \xi_{u>0} \nabla u$$

with $\xi_{u>0}$ *being the characteristic Function on* $\{u > 0\} = \{x \in \Omega : u(x) > 0\}$*. Furthermore* $\nabla u = 0$ *a.e. in* $\{u = 0\} = \{x \in \Omega : u(x) = 0\}$*[29].*

Lemma A.13 (Stampacchia)**:** *Let* $C > 0, \alpha > 0, \beta > 1 \in \mathbb{R}$ *and F be a function from* $\mathbb{R} \to \mathbb{R}$*. Let further F fulfill the following inequality for some* k_0

$$F(h) \leqslant \frac{C^\alpha}{(h-k)^\alpha} F(k)^\beta \quad \forall h > k \geqslant k_0.$$

Then $F(h) = 0$ *for* $h \geqslant k_0 + k^*$ *with* $k^* := C 2^{\frac{\beta}{\beta-1}} F(k_0)^{\frac{\beta-1}{\alpha}}$*[30].*

BIBLIOGRAPHY

[1] Jens Markus Melenk. *Lecture notes on: Numerik partieller Differentialgleichungen: stationäre Probleme*. 2014. URL: http://www.asc.tuwien.ac.at/~melenk/teach/fem_WS1314/.

[2] W Sparreboom, A Van Den Berg, and JCT Eijkel. "Principles and applications of nanofluidic transport." In: *Nature nanotechnology* 4.11 (2009), pp. 713–720.

[3] RK Joshi, Paola Carbone, Feng-Chao Wang, Vasyl G Kravets, Ying Su, Irina V Grigorieva, HA Wu, Andre K Geim, and Rahul Raveendran Nair. "Precise and ultrafast molecular sieving through graphene oxide membranes." In: *Science* 343.6172 (2014), pp. 752–754.

[4] Jongyoon Han, Jianping Fu, and Reto B Schoch. "Molecular sieving using nanofilters: past, present and future." In: *Lab on a Chip* 8.1 (2008), pp. 23–33.

[5] Mubarak Ali, Basit Yameen, Reinhard Neumann, Wolfgang Ensinger, Wolfgang Knoll, and Omar Azzaroni. "Biosensing and supramolecular bioconjugation in single conical polymer nanochannels. Facile incorporation of biorecognition elements into nanoconfined geometries." In: *Journal of the American Chemical Society* 130.48 (2008), pp. 16351–16357.

[6] Martin Burger, Bärbel Schlake, and Marie T Wolfram. "Nonlinear Poisson–Nernst–Planck equations for ion flux through confined geometries." In: *Nonlinearity* 25.4 (2012), p. 961. URL: http://iopscience.iop.org/article/10.1088/0951-7715/25/4/961.

[7] Bärbel Angelika Schlake. "Mathematical models for particle transport: Crowded motion." PhD thesis. Westfälische Wilhelms-Universität Münster, 2011. URL: http://wwwmath.uni-muenster.de/num/inst/natterer/Arbeitsgruppen/ag_burger/organization/schlake/DissBS.pdf.

[8] Dirk Gillespie, Wolfgang Nonner, and Robert S Eisenberg. "Coupling Poisson–Nernst–Planck and density functional theory to calculate ion flux." In: *Journal of Physics: Condensed Matter* 14.46 (2002), p. 12129. URL: http://iopscience.iop.org/article/10.1088/0953-8984/14/46/317.

[9] Walther Nernst. "Zur kinetik der in lösung befindlichen körper." In: *Z. phys. Chem* 2 (1888), p. 613.

[10] Walther Nernst. "Die elektromotorische Wirksamkeit von Ionen." In: *Z. phys. Chem* 4 (1889).

[11] Walther Nernst. "Zur Theorie der elektrischen Reizung." In: *Nachrichten von der Gesellschaft der Wissenschaften zu Göttingen, Mathematisch-Physikalische Klasse* 1899 (1899), pp. 104–108.

[12] Max Planck. "Über die Erregung von Elektrizität und Wärme in Elektrolyten." In: *Ann. der Phys. und Chem.* 39 (1890), pp. 161–186.

[13] Luigi Ambrosio, Nicola Gigli, and Giuseppe Savaré. *Gradient flows: in metric spaces and in the space of probability measures*. Springer Science & Business Media, 2008.

[14] Giambattista Giacomin and Joel L Lebowitz. "Phase segregation dynamics in particle systems with long range interactions. I. Macroscopic limits." In: *Journal of statistical Physics* 87.1-2 (1997), pp. 37–61. URL: http://link.springer.com/article/10.1007/BF02181479.

[15] Gonzalo Galiano, Ansgar Jüngel, and Julián Velasco. "A parabolic cross-diffusion system for granular materials." In: *SIAM Journal on Mathematical Analysis* 35.3 (2003), pp. 561–578. URL: http://epubs.siam.org/doi/abs/10.1137/S0036141002409386.

[16] Li Chen and Ansgar Jüngel. "Analysis of a multidimensional parabolic population model with strong cross-diffusion." In: *SIAM journal on mathematical analysis* 36.1 (2004), pp. 301–322. URL: http://epubs.siam.org/doi/abs/10.1137/S0036141003427798.

[17] Marco Di Francesco, Klemens Fellner, and Peter A Markowich. "The entropy dissipation method for spatially inhomogeneous reaction–diffusion-type systems." In: *Proceedings of the Royal Society of London A: Mathematical, Physical and Engineering Sciences*. Vol. 464. 2100. The Royal Society. 2008, pp. 3273–3300. URL: http://rspa.royalsocietypublishing.org/content/464/2100/3273.short.

[18] Bertil Hille et al. *Ion channels of excitable membranes*. Sinauer Sunderland, MA, 2001.

[19] Olga-A Ladyzhenskaya, Nina-N Ural'tseva, and Leon Ehrenpreis. *Linear and quasilinear elliptic equations*. Academic Press, Collier-Macmillan Ltd., 1968.

[20] David Gilbarg and Neil S Trudinger. *Elliptic partial differential equations of second order*. Springer, 1983.

[21] Rainer Ansorge and W Törnig. *Numerische Lösung nichtlinearer partieller Differential-und Integrodifferentialgleichungen: Vorträge einer Tagung im Mathematischen Forschungsinstitut Oberwolfach, 1971*. Vol. 267. Springer-Verlag, 2006.

[22] Douglas Arnold. *Lecture notes on: Numerical Analysis of Partial Differential Equations*. 2015. URL: https://www.ima.umn.edu/~arnold/8445-8446.14-15/notes.pdf.

[23] Martin Bluemlinger. "Lecture notes on: Satz von Eberlein-Smulian." In: (2015). URL: http://www.asc.tuwien.ac.at/~blue/Eb-Smu.pdf.

[24] Norbert Kusolitsch. *Maß-und Wahrscheinlichkeitstheorie: Eine Einführung*. Springer-Verlag, 2014.

[25] Anton Arnold. *Lecture notes on: Nichtlineare Partielle DIfferentialgleichungen*. 2013. URL: http://www.asc.tuwien.ac.at/~arnold/lehre/nlpdgl/NLpDiff.pdf.

[26] Anton Arnold. *Lecture notes on: Variationsrechnung*. 2016. URL: http://www.asc.tuwien.ac.at/~arnold/lehre/variationsrechnung/var-rechn.pdf.

[27] Giovanni Maria Troianiello. *Elliptic differential equations and obstacle problems*. Springer Science & Business Media, 2013.

[28] Lawrence C. Evans. *Partial differential equations*. Graduate studies in mathematics. American Mathematical Society, 1998.

[29] Ansgar Juengel. *Lecture notes on: Nichtlineare Partielle Differentialgleichungen*. 2016. URL: http://www.asc.tuwien.ac.at/~juengel/scripts/nPDE.pdf.

[30] G Stampacchia. "Equations elliptiques du second ordre a coefficients discontinus." In: *Les Presses de l'Universite de Montreal* 15501 (1966).